The Cryosphere Discuss., 8, 4959–5013, 2014
www.the-cryosphere-discuss.net/8/4959/2014/
doi:10.5194/tcd-8-4959-2014

The Cryosphere Discussions
Open Access

Site-level model intercomparison of high latitude and high altitude soil thermal dynamics in tundra and barren landscapes

A. Ekici[1], S. Chadburn[2], N. Chaudhary[3], L. H. Hajdu[4], A. Marmy[5], S. Peng[6,7], J. Boike[8], E. Burke[9], A. D. Friend[4], C. Hauck[5], G. Krinner[6], M. Langer[6,8], P. A. Miller[3], and C. Beer[10]

[1]Department of Biogeochemical Integration, Max Planck Institute for Biogeochemistry, Jena, Germany
[2]College of Engineering, Mathematics and Physical Sciences, University of Exeter, Exeter, UK
[3]Department of Physical Geography and Ecosystem Science, Lund University, Lund, Sweden
[4]Department of Geography, University of Cambridge, Cambridge, UK
[5]Department of Geosciences, University of Fribourg, Fribourg, Switzerland
[6]Laboratoire de Glaciologie et Géophysique de l'Environnement, CNRS and Université Grenoble Alpes, LGGE, 38041, Grenoble, France
[7]Laboratoire des Sciences du Climat et de l-Environnement (LSCE), UMR CEA-CNRS, Batîment 709, CE, L'Orme des Merisiers, 91191 Gif-sur-Yvette, France

[8]Alfred-Wegener-Institut, Helmholtz-Zentrum für Polar- und Meeresforschung, Potsdam, Germany
[9]Met Office Hadley Centre, Exeter, UK
[10]Department of Applied Environmental Science (ITM) and Bolin Centre for Climate Research, Stockholm University, Stockholm, Sweden

Received: 8 July 2014 – Accepted: 6 September 2014 – Published: 18 September 2014

Correspondence to: A. Ekici (aekici@bgc-jena.mpg.de)

Published by Copernicus Publications on behalf of the European Geosciences Union.

Abstract

Modelling soil thermal dynamics at high latitudes and altitudes requires representations of specific physical processes such as snow insulation, soil freezing/thawing, as well as subsurface conditions like soil water/ice content and soil texture type. We have compared six different land models (JSBACH, ORCHIDEE, JULES, COUP, HYBRID8, LPJ-GUESS) at four different sites with distinct cold region landscape types (i.e. Schilthorn-Alpine, Bayelva-high Arctic, Samoylov-wet polygonal tundra, Nuuk-non permafrost Arctic) to quantify the importance of physical processes in capturing observed temperature dynamics in soils. This work shows how a range of models can represent distinct soil temperature regimes in permafrost and non-permafrost soils. Snow insulation is of major importance for estimating topsoil conditions and must be combined with accurate subsoil temperature dynamics to correctly estimate active layer thicknesses. Analyses show that land models need more realistic surface processes (such as detailed snow dynamics and moss cover with changing thickness/wetness) as well as better representations of subsoil thermal dynamics (i.e. soil heat transfer mechanism and correct parameterization of heat conductivity/capacities).

1 Introduction

Recent atmospheric warming trends are affecting terrestrial systems by increasing soil temperatures and causing changes in the hydrological cycle. Especially in high latitudes/altitudes, clear signs of change are observed (Serreze et al., 2000; ACIA, 2005; IPCC AR5, 2013). These relatively colder regions are characterized by the frozen state of terrestrial water, which makes soils more vulnerable to warming by bringing the risk of shifting them into an unfrozen state. Such changes will have broad implications for the physical (Romanovsky, 2010), biogeochemical (Schuur et al., 2008) and structural (Larsen et al., 2008) conditions of the local, regional as well as global climate system.

TCD
8, 4959–5013, 2014

Therefore, predicting the future state of the soil thermal regime at high latitudes and altitudes holds major importance for Earth system modelling.

There are increasing concerns as to how land models perform at capturing high latitude soil thermal dynamics, in particular in permafrost regions. Recent studies (Koven et al., 2013; Slater and Lawrence, 2013) have provided detailed assessments of commonly used Earth System Models (ESMs) in simulating soil temperatures of present and future state of the Arctic. By using the Coupled Model Intercomparison Project phase 5 – CMIP5 (Taylor et al., 2009) results, Koven et al. (2013) have shown a broad range of model outputs in estimating soil temperature. They attributed most of the intermodel discrepancies to air–land surface coupling and snow representations in models. Similar to those findings, Slater and Lawrence (2013) confirmed the high uncertainty of CMIP5 models in predicting the permafrost state and their future trajectories. They have concluded that the analyzed versions of models are not appropriate for such experiments since they lack critical processes for cold region soils. Out of the many potential reasons, snow insulation, land model physics, and vertical model resolutions were identified as being the major sources of uncertainty.

Current land surface schemes and most of the vegetation and soil models represent energy and mass exchange between the land surface and atmosphere in one dimension. Using a grid cell approach, such exchanges are estimated for the entire land surface or specific regions. Therefore, comparing simulated and observed time series of states or fluxes at point scale rather than grid averaging, is an important component of model evaluation in order to understand remaining limitations of models (Ekici et al., 2014; Mahecha et al., 2010). In such "site-level runs", we assume that lateral processes do not influence the observations. Then, models are driven by observed climate and variables of interest can be compared to observations at different temporal scales. Even though such idealized field conditions never exist, a careful interpretation of site-level runs can identify major gaps in process representations in models.

In recent years, land models have improved their representations of the soil physical environment in cold regions. Model enhancements include the addition of soil freezing/thawing, detailed snow representations, prescribed moss cover, extending soil columns, and coupling soil heat transfer with hydrology (Ekici et al., 2014; Gouttevin et al., 2012a; Dankers et al., 2011; Lawrence et al., 2008; Wania et al., 2009a). Such improvements highlight the need for an updated assessment of model performances in representing high latitude/altitude soil thermal dynamics.

We have compared the performances of six different land models in simulating soil thermal dynamics at four contrasting sites. In comparison to previous works (Koven et al., 2013; Slater and Lawrence, 2013), we used advanced model versions specifically improved for cold regions and our model simulations are driven by (and evaluated with) site observations. To represent a wider range of assessment and model structures, we used both land components of ESMs (JSBACH, ORCHIDEE, JULES) and stand-alone models (COUP, HYBRID8, LPJ-GUESS), and compared them at Arctic permafrost, Alpine permafrost and Arctic non-permafrost sites. By doing so, we aimed to quantify the importance of different processes, to determine the general shortcomings of current model versions and finally to highlight the key processes for future model developments.

2 Methods

2.1 Model descriptions

2.1.1 JSBACH

Jena Scheme for Biosphere–Atmosphere Coupling in Hamburg (JSBACH) is the land surface component of the Max Planck Institute Earth System Model (MPI-ESM) that comprise ECHAM6 for the atmosphere (Stevens et al., 2012) and MPIOM for the ocean (Jungclaus et al., 2013). It provides the land surface boundary for the atmosphere in coupled simulations; however, it can also be used offline driven by atmospheric forcing. The current version of JSBACH (Ekici et al., 2014) employs soil heat transfer coupled to

TCD
8, 4959–5013, 2014

hydrology with freezing and thawing processes included. The soil model is discretized as five layers with increasing thicknesses up to 10 m depth. There are up to 5 snow layers with constant density and heat transfer parameters. JSBACH also simulates a simple moss/organic matter insulation layer again with constant parameters.

2.1.2 ORCHIDEE

ORCHIDEE is a land surface model, which can be used coupled to the IPSL-GCM or driven offline by prescribed atmospheric forcing (Krinner et al., 2005). ORCHIDEE computes all the soil–atmosphere–vegetation relevant energy and water exchange processes in 30 min time steps. It combines a soil–vegetation–atmosphere transfer model with a carbon cycle module computing vertically detailed soil carbon dynamics. The high latitude version of ORCHIDEE includes a dynamic three-layer snow module (Wang et al., 2013), soil freeze–thaw processes (Gouttevin et al., 2012a), and a vertical permafrost soil thermal and carbon module (Koven et al., 2011). The soil hydrology is vertically discretized as 11 numerical nodes with 2 m depth (Gouttevin et al., 2012a), and soil thermal and carbon modules are vertically discretized as 32 layers with ~ 47 m depth (Koven et al., 2011). One-dimensional Fourier equation was applied to calculate soil thermal dynamics, and both soil thermal conductivity and heat capacity are functions of the fraction of frozen and unfrozen soil water content and dry, saturated soil thermal properties (Gouttevin et al., 2012b).

2.1.3 JULES

JULES (Joint UK Land Environment Simulator) is the land-surface scheme used in the Hadley Centre climate model (Best et al., 2011; Clark et al., 2011), which can also be run offline, driven by atmospheric forcing data. It is based on the Met Office Surface Exchange Scheme, MOSES (Cox et al., 1999). JULES simulates surface exchange, vegetation dynamics and soil physical processes. It can be run at a single point, or as a set of points representing a 2-D grid. In each grid cell, the surface is tiled into

TCD
8, 4959–5013, 2014

different surface types, and the soil is treated as a single column, discretized vertically into layers (4 in the standard set-up). JULES simulates fluxes of moisture and energy between the atmosphere, surface and soil, and the soil freezing and thawing. It includes a carbon cycle that can simulate carbon exchange between the atmosphere, vegetation and soil. It also includes a multi-layer snow model (Best et al., 2011), with layers that have variable thickness, density and thermal properties. The snow scheme significantly improves the soil thermal regime in comparison with the old, single-layer scheme (Burke et al., 2013). The model can be run with a timestep of between 30 min and 3 h, depending on user preference.

2.1.4 COUP

COUP is a stand-alone, one-dimensional heat and mass transfer model for the soil–snow–atmosphere system (Jansson and Karlberg, 2011) and is capable of simulating transient hydrothermal processes in the subsurface including seasonal or perennial frozen ground (see e.g. Hollesen et al., 2011; Scherler et al., 2010, 2013). Two coupled partial differential equations for water and heat flow are the core of the COUP Model. They are calculated over up to 50 vertical layers of arbitrary depth. Processes that are important for permafrost simulations, such as freezing and thawing of the soil as well as the accumulation, metamorphosis, and melt of a snow cover are included in the model (Lundin, 1990; Gustafsson et al., 2001). At temperatures above a threshold temperature (–6 °C), unfrozen water coexists with ice. This approach respects the fact that in porous media, liquid water coexists with frozen water at temperatures far below freezing point, due to high pressure build up inside small pore spaces during freezing (Anderson et al., 1973). Freezing processes in the soil are based on a function of freezing point depression and on an analogy of freezing-thawing and wetting-drying (Harlan, 1973; Jansson and Karlberg, 2011). Snow cover is simulated as one layer of variable height, density, and water content.

The upper boundary condition is given by a surface energy balance at the soil–snow–atmosphere boundary layer, driven by air temperature, relative humidity, wind speed, global radiation, incoming longwave radiation and precipitation. The lower boundary condition at the bottom of the soil column is usually given by the geothermal heat flux (or zero heat flux) and a seepage flow of percolating water. Water transfer in the soil depends on texture, porosity, water, and ice content. Bypass flow through macropores, lateral runoff and rapid lateral drainage due to steep terrain can also be considered (e.g. Scherler et al., 2013). A detailed description of the model including all its equations and parameters is given in Jansson and Karlberg (2011) and Jansson (2012).

2.1.5 HYBRID8

HYBRID8 is a stand-alone land surface model, which computes the carbon and water cycling within the biosphere and between the biosphere and atmosphere. It is driven by the daily/sub-daily climate variables above the canopy, and the atmospheric CO_2 concentration. Computations are performed on a 30 min timestep for the energy fluxes, exchanges of carbon and water with the atmosphere and the soil. Litter production and soil decomposition are calculated at a daily timestep. HYBRID8 uses the surface physics and the latest parameterization of turbulent surface fluxes from the GISS ModelE (Schmidt et al., 2006), but has no representation of vegetation dynamics. Also the snow dynamics from modelE are not yet fully incorporated. Heat dynamics are described in Rosenzweig et al. (1997) and moisture dynamics in Abramopoulos et al. (1998).

In HYBRID8 the prognostic variable for the heat transfer is the heat in the different soil layers and from that the model evaluates the soil temperature. The processes governing this are the diffusion from the surface to the different layers, as atmospheric forcing, and the conduction and advection between the soil layers. The bottom boundary layer in HYBRID8 is impermeable resulting in zero heat flux from below soil layers. The version used in this project has no representation of the snow dynamics and has no insulating vegetation cover.

TCD
8, 4959–5013, 2014

2.1.6 LPJ-GUESSS

LPJ-GUESS (Lund–Potsdam–Jena General Ecosystem Simulator; Smith et al., 2001) is a process-based model of vegetation dynamics and biogeochemistry optimized for regional and global applications. Mechanistic representations of biophysical and biogeochemical processes are shared with those in the Lund–Potsdam–Jena dynamic global vegetation model LPJ-DGVM (Sitch et al., 2003; Gerten et al., 2004). However, LPJ-GUESS replaces the large area parameterization scheme in LPJ-DGVM, whereby vegetation is averaged out over a larger area allowing several state variables to be calculated in a simpler and faster manner, with more robust and mechanistic schemes of individual- and patch-based resource competition and woody plant population dynamics. Detailed descriptions are given by Smith et al. (2001), Sitch et al. (2003), Wolf et al. (2008), Miller and Smith (2012), and Zhang et al. (2013).

LPJ-GUESS has recently been updated to simulate Arctic upland and peatland ecosystems (McGuire et al., 2012; Zhang et al., 2013). It shares the numerical soil thawing-freezing processes, peatland hydrology and the model of wetland methane emission with LPJ-DGVM WHyMe, as described by Wania et al. (2009a, b, 2010). To simulate soil temperatures and active layer depths, the soil column in LPJ-GUESS is divided into a single snow layer of fixed density and variable thickness, a litter layer of fixed thickness (10 cm for these simulations, except for Schilthorn where it is set to 2.5 cm), a soil column of 2 m depth (with sublayers of thickness 0.1 m, each with a prescribed fraction of mineral and organic material, but with fractions of soil water and air that are updated daily), and finally a "padding" column of depth 48 m (with thicker sublayers), to simulate soil thermal dynamics. Insulation effects of snow, phase changes in soil water, daily precipitation input and air temperature forcing are important determinants of daily soil temperature dynamics at different sub-layers.

TCD
8, 4959–5013, 2014

2.2 Study sites

2.2.1 Nuuk

The Nuuk observational site is located at southwestern Greenland. The site is situated in the Kobbefjord at 500 m altitude a.s.l. and ambient conditions show arctic/polar climate properties with a mean annual temperature of −1.5 °C in 2008 and −1.3 °C in 2009 (Jensen and Rasch, 2009, 2010). Vegetation types consists of Empetrum nigrum with Betula nana and Ledum groenlandicum with a vegetation height of 3–5 cm. The study site soil lacks mineral soil horizons due to cryoturbation and lack of podsol development as it is placed on a dry location. Soil is composed of 43 % sand, 34 % loam, 13 % clay and 10 % organic materials. No soil ice or permafrost formations have been observed within the drainage basin. Snow cover is measured at the Climate Basic station 1.65 km from the soil station but at the same altitude. At the time of the annual Nuuk Basic snow survey in mid-April, the snow depth at the soil station was very similar to the snow depth at the Climate Basic station: ±0.1 m when the snow depth is high (near 1 m). Strong winds (> 20 m s^{-1}) have a strong influence on the redistribution of newly fallen snow especially in the beginning of the snow season, so the formation of a permanent snow cover at the soil station can be delayed as much as one week, while the end of the snow cover season it is similar to that at the Climate Basic station (B. U. Hansen, personal communication, 2013).

2.2.2 Schilthorn

The Schilthorn massif (Bernese Alps, Switzerland) is situated at 2970 m altitude in the north central part of the European Alps, and its non-vegetated lithology is dominated by deeply weathered limestone schists forming a surface layer of mainly sandy and gravelly debris up to 5 m thick over presumably strongly jointed bedrock. Following the first indications of permafrost (ice lenses) during the construction of the summit station between 1965 and 1967, the site was chosen for long-term permafrost observation within the framework of the European PACE project and consequently integrated into the Swiss permafrost monitoring network PERMOS as one of its reference sites (PERMOS, 2013).

The measurements at the monitoring station at 2900 m altitude are located on a flat plateau on the north-facing slope and comprise a meteorological station and three boreholes (14 m vertical, 100 m vertical and 100 m inclined) with continuous ground temperature measurements since 1999 (Vonder Mühll et al., 2000; Hoelzle and Gruber, 2008; Harris et al., 2009). Borehole data indicate permafrost of at least 100 m thickness, which is characterized by ice-poor conditions close to the melting point. Maximum active-layer depths recorded since the start of measurements in 1999 are generally around 4–6 m, but during the exceptionally warm summer of the year 2003 the active-layer depth increased to 8.6 m, reflecting the potential for degradation of this warm permafrost site (Hilbich et al., 2008).

The monitoring station is complemented by soil moisture measurements since 2007 and geophysical (mainly geoelectrical) monitoring since 1999 (Hauck, 2002; Hilbich et al., 2011). The snow cover at the Schilthorn can reach maximum depths of about 2–3 m and usually lasts from October through to June/July. One dimensional soil model sensitivity studies showed that, caused by this late snowmelt and the long decoupling of the atmosphere from the surface, impacts of long-term atmospheric changes would be strongest in summer and autumn, when continuously increasing air temperatures could lead to a severe increase in active-layer thickness (Engelhardt et al., 2010; Marmy et al., 2013; Scherler et al., 2013).

2.2.3 Samoylov

Samoylov Island belongs to an alluvial river terrace of the Lena River Delta. The island is elevated about 20 m above the normal river water level and covers an area of about 3.4 km^2 (Boike et al., 2013). The western part of the island constitutes a modern floodplain which is lowered compared to the rest of the island and is often flooded during ice break-up of the Lena River in spring. The eastern part of the island belongs to the elevated river terrace, which is mainly characterized by moss, and sedge vegetated tundra (Kutzbach et al., 2007). In addition, several lakes and ponds occur which make up about 25 % of the surface area of Samoylov (Muster et al., 2012). The land surface of the island is characterized by the typical micro-relief of polygonal patterned ground caused by frost cracking and subsequent ice-wedge formation. The polygonal structures usually consist of depressed centers, which are surrounded by elevated rims. The polygonal structures often occur in different stages of degradation with partly to completely collapsed rims (Kutzbach et al., 2007). The soil in the polygonal centers usually consists of water saturated sandy peat with the water table standing a few centimeters below or above the surface. The elevated rims are usually covered with a dry moss layer underlain by wet sandy soils with massive ice wedges underneath. The cryogenic soil complex of the river terrace reaches depths of 10 to 15 m and is underlain by sandy to silty river deposits. The deposits of the Lena River reach depths of at least 1 km in the delta region (Langer et al., 2013).

There are strong spatial differences in surface energy balance due to highly fractionated surface and subsurface properties. Due to thermo-erosion, there is an expansion of thermokarst lakes and small ponds (Abnizova et al., 2012). Soil water drainage is strongly related to active layer dynamics, lateral water flow occurs from late summer to autumn (Helbig et al., 2012). Site conditions include strong snow-micro-topography, snow-vegetation interactions due to wind drift (Boike et al., 2013).

2.2.4 Bayelva

The Bayelva climate and soil-monitoring site is located in the Kongsfjord region at the west coast of the Svalbard Island. The North Atlantic Current warms this area to an average air temperature of about −13 °C in January and +5 °C in July, and provides about 400 mm precipitation annually, falling mostly as snow between September and May. The annual mean temperature of 1994 to 2010 in Ny-Ålesund has been increasing by +1.3 K decade^{-1} Maturilli et al. (2013). The observation site is located in the Bayelva River catchment on the Brøgger peninsula, about 3 km from the village of

Ny-Ålesund. The Bayelva catchment is bordered by two mountains, the Zeppelinfjellet and the Scheteligfjellet, between which the glacial Bayelva River originates from the two branches of the Brøggerbreen glacier moraine rubble. To the north of the study site, the terrain is flattening and at about 1 km distance the Bayelva River reaches the shoreline of the Kongsfjorden (Arctic Ocean). In the catchment area, sparse vegetation alternates with exposed soil and sand and rock fields. Typical permafrost features, such as mud boils and non-sorted circles, are found in many parts of the study area. The Bayelva permafrost site itself is located at 25 m a.s.l., on top of the small Leirhaugen hill. The dominant ground pattern at the study site consists of non-sorted soil circles. The bare soil circle centers are about 1 m in diameter and are surrounded by a vegetated rim consisting of a mixture of low vascular plants of different species of grass and sedges (*Carex* spec., *Deschampsia* spec., *Eriophorum* spec., *Festuca* spec., *Luzula* spec.), catchfly, saxifrage, willow and some other local common species (*Dryas octopetala*, *Oxyria digyna*, *Polegonum viviparum*) and unclassified species of mosses and lichens. The vegetation cover at the measurement site was estimated to be approximately 60 %, with the remainder being bare soil with a small proportion of stones. The silty clay soil has a high mineral content, while the organic content is low, with organic fractions below 10 % (Boike et al., 2007). In the study period, the permafrost at Leirhaugen hill had a mean annual temperature of about −2 °C at the top of the permafrost at 1.5 m depth.

Over the past decade the Bayelva catchment has been the focus of intensive investigations into soil and permafrost conditions (Roth and Boike, 2001; Boike et al., 2007; Westermann et al., 2010, 2011), the winter surface energy balance (Boike et al., 2003), and the annual balance of energy, H_2O and CO_2 and micrometeorological processes controlling these fluxes (Westermann et al., 2009; Lüers et al., 2014).

2.3 Intercomparison set-up and simulation protocol

In order to compare solely model representations of physical processes and eliminate any other source of uncertainty (e.g. climate forcing, spatial resolution, soil parameters etc.), model simulations are standardized as much as possible. Driving data for all site simulations were prepared and distributed uniformly. Site observations were converted into continuous time series with minor gap filling. Where the observed variable set lacked the variable needed by the models, extended WATCH reanalysis data (Weedon et al., 2010; Beer et al., 2014) was used to complement the data sets. Soil thermal properties are based on the sand, silt, and clay fractions of the Harmonized World Soil database v1.1 (FAO et al., 2009). All model simulations are forced with these datasets and the outputs from these site-level offline simulations are analyzed in this paper. Table 3 summarizes the details of site driving data preparation together with soil static parameters. To bring the state variables into equilibrium with climate, models are spun up with climate forcing and the details are given in Table 4.

Most of the comparisons are performed for the upper part of the soil. The term "topsoil" is referred from now on to indicate the chosen upper soil layer in each model and the first depth of soil temperature observations. The details of layer selection are given in Table A1.

3 Results and discussions

3.1 Topsoil temperature and insulation effects

Estimating site-level soil temperature using global models is quite challenging yet valuable for process understanding. Driven by observed atmospheric conditions at the sites, off-line model simulations can be used for comparison to observed soil temperature. Figure 1 shows average seasonal topsoil temperature (see Table A1) distributions extracted from the six models as well as the observed values at the four different sites. As all our study sites are located in cold climate zones, there is significant seasonality, which requires analyzing each season separately and inspecting key seasonal processes. In this figure, simulated temperatures show a wide range of values depending on site-specific conditions and model formulations. Winter and spring comparisons have larger biases than summer and autumn (Fig. 1). However, summer comparison also shows considerable deviations from the observations as well as among models. Observed winter and spring temperatures are much colder at Samoylov than the other sites. Also there is a bigger range of temperature distribution at this site. However, observed summer temperatures are similar at all sites, although the non-permafrost Nuuk site has warmer conditions than the others. For the modeled values, there is higher inconsistency in capturing observed winter temperatures, especially at Samoylov and Schilthorn. Additionally the modeled temperature range increases in spring. Even though the mean modeled temperatures are closer to observed means in summer, the max and min values show a wide range of values during this season. Autumn, however, shows a more uniform distribution of temperatures compared to other seasons. A proper assessment of critical processes entails examining seasonal changes in surface cover and its consequent insulation effects for the topsoil temperature, which will be presented in the following.

Modeling soil heat transfer requires accurate coupling of atmosphere and soil. Vegetation cover, snow pack, litter layers, organic layer or a combination of these can form a buffer zone at this interface. This buffer zone provides thermal insulation for soil. Especially at high latitudes/altitudes, where soil is snow-covered during most of the year, insulation effects are critical for estimating the soil thermal regime as well as the active layer thickness and permafrost conditions. As has been shown in a number of studies (e.g. Koven et al., 2013; Scherler et al., 2013; Gubler et al., 2013; Fiddes et al., 2013) modeled mean soil temperatures are strongly related to the atmosphere–surface thermal connection, which is strongly influenced by snow cover and its properties. Snow cover can increase the mean annual ground temperature and reduce the seasonal freezing depth (Zhang, 2005). However, the combined effects of snow cover and vegetation insulation together with soil organic content is needed to accurately estimate soil temperatures (Schaefer et al., 2009).

Figure 2 shows the seasonal relations between air and topsoil temperature at each study site. In this figure, soil temperature values vary for each model with the same

TCD
8, 4959–5013, 2014

air temperature value, as all models are driven with the same atmospheric forcing. When snow insulation protects the topsoil from cooling, values lay above the 1 : 1 line. During the snow free season, when only vegetation cover, litter layers or organic layer insulation protects the topsoil from warming, values stay below the 1 : 1 line. However, insulation strength can change dramatically with critical levels of snow depth or dryness of the vegetation cover. Aside from the insulation effects, the relation between air and topsoil temperature depends also on atmosphere/topsoil temperature gradient, soil type/wetness and subsoil temperatures.

The site observations show warmer topsoil temperatures than air during autumn, winter and spring (Fig. 2). This situation indicates that soil is insulated when compared to colder air temperatures. This can be attributed to the snow cover during these seasons (Fig. 3). High insulating property of snow keeps the soil warmer than air, while not having snow usually results in colder topsoil temperatures than air (as for the HYBRID8 model, cf. Fig. 2). Even though the high albedo of snow provides a cooling effect for soil, the warming due to insulation dominates during most of the year. As discussed above, winter temperatures show the biggest deviations between models and observations. Spring and autumn have almost the same pattern with a reduced range. However, summer modeled temperatures are much closer with each other, but their location w.r.t. 1 : 1 line is not consistent.

Depending on their snow depth bias, models show different relations between air and topsoil temperature. Figure 3 shows the changes in snow depth from observed and modeled values. Compared to observations, the models that underestimate the snow depth at Nuuk and Bayelva (Fig. 3a and d) show colder topsoil temperature values in winter and are closer to the 1 : 1 line in Fig. 2. On the other hand, the amount of winter warm bias from snow depth overestimation in models depends on whether the site has a "sub- or supra-critical" snow height. With supra-critical conditions (e.g. at Schilthorn), the snow depth is so high that a small over/underestimation of the model does not make a difference regarding the insulation. Only the timing of the snow arrival and melt-out is important. In sub-critical conditions (e.g. at Samoylov), the snow depth is so low

TCD
8, 4959–5013, 2014

that every overestimation leads automatically to a strong warm bias in the simulation e.g. for JULES/COUP. This effect is also mentioned in Zhang (2005), where it is stated that snow depths of less than 50 cm has the greatest impact on soil temperatures. However, overestimated snow depth at Samoylov and Schilthorn does not always result in warmer soil temperatures in models as expected (Fig. 2b and c). At these sites, even though JSBACH, JULES and COUP show warmer soil temperatures in parallel to their snow depth overestimations, ORCHIDEE and LPJ-GUESS show the opposite. This behavior indicates different processes working in opposite ways.

Nevertheless, most of winter, autumn and spring topsoil temperature biases can be explained by snow conditions. For our study sites, the amount of snow depth bias is correlated with the amount of topsoil temperature bias (Fig. 4). With overestimated (underestimated) snow depth, models generally simulate warmer (colder) topsoil temperatures. As seen in Fig. 4a, almost all models underestimate the snow depth at Nuuk and Bayelva, and this created colder topsoil temperatures. However, the overestimation of snow depth usually leads to warmer topsoil temperatures, but other processes can compensate the warming and create a colder topsoil temperature (ORCHIDEE and LPJ-GUESS values in Fig. 4 samoylov and Schilthorn sites). Figure 4b shows that snow depth bias can explain the topsoil temperature bias even when the snow free season is considered, which is due to the long snow period at these sites (Table 2). This confirms the importance of snow representation in models for capturing topsoil temperatures at high latitudes and high altitudes.

However, considering dynamic heat transfer parameters (volumetric heat capacity and heat conductivity) in snow representation seems to be of lesser importance (JSBACH vs. other models, see Table 1). This is related to the fact that most global models generally lack other important site-specific snow processes such as strong wind drifts (creating patchy snow cover), depth hoar formation and snow metamorphism (changing snow pack properties), snowmelt water infiltration into soil (additional heat transfer mechanism) and snow albedo changes with these processes. As an example, the landscape heterogeneity at Samoylov forms different soil thermal profiles for polygon center and rim. While the soil temperature comparisons were performed for the polygon rim, snow depth observations were taken from polygon center. Due to strong wind drift almost all snow is removed from the rim and also limited to ca. 50 cm (average polygon height) at the center (Boike et al., 2008). This way, models are forced to overestimate snow depth and insulation, in particular on the rim where soil temperature measurements have been taken. Hence, a resulting winter warm bias is no surprise (Fig. 1a, models JSBACH, JULES, COUP).

After snowmelt, surface vegetation cover and organic layer form the buffer zone at the atmosphere/soil interface. Insulating properties of vegetation cover depend on the type of species, its thickness and wetness of the layer. In our study sites (except for the bare Schilthorn site), vegetation comprise of moss cover with ca. 5–15 cm thickness. Increasing thickness changes the heat storage of the moss cover and acts as a stronger insulator (Gornall et al., 2007). Additionally, water content of the moss layer affects the heat transfer parameters (Soudzilovskaia et al., 2013). Transition from frozen to thawed state decreases the heat conductivity and increases the heat capacity of moss layer (due to large differences between ice and liquid water); however, loss of moisture allows more air in the moss mat and thus decreases the heat conductivity of the layer (due to much lower heat conductivity of air). Therefore, composition of the moss layer can strongly affect its insulation strength.

During summer, observed values show warmer topsoil temperatures than air at Nuuk and Bayelva, while the opposite is seen at Schilthorn and Samoylov (Fig. 2). Thicker moss cover and higher moisture content at Samoylov (Boike et al., 2008) is the reason for better insulation (hence cooler summer topsoil temperatures) at this site. However, without any plant cover, the cooler topsoil temperatures at Schilthorn point to non-vegetation induced insulation in summer. As snow can be persistent over spring season at high latitudes/altitudes and does not completely disappear in summer months (Fig. 3), it is worthwhile to separate snow and snow free seasons for these comparisons. Figure 5 shows the same atmosphere/topsoil temperature comparison as in Fig. 2 but using snow and snow free seasons instead of conventional seasons.

TCD
8, 4959–5013, 2014

Evidently, without snow cover, the Schilthorn site indeed has warmer topsoil temperatures than air as expected (Fig. 5b).

During the snow free period, the insulation effects of the vegetation cover and litter/organic layer are seen (Fig. 5). Compared to the snow-covered period, observed values are closer to the 1 : 1 line, implying that the insulation is smaller during this season. The models generally agree with this observation (Fig. 5), but their relations to the observed values are inconsistent with each other at all sites except Bayelva. At this site, all models underestimate the observed topsoil temperatures all year long (Fig. 5d). With underestimated snow depth (Fig. 3d) and winter cold bias in topsoil temperature (Fig. 2d), models create a colder soil thermal profile that results in cooling of the surface from below even during the snow free season. Furthermore, using global reanalysis product instead of site observations (Table 3) might cause biases in incoming longwave radiation, which can also affect the soil temperature calculations. In order to assess the model performance in capturing observed soil temperature dynamics, it is important to drive the models with a complete set of site observations.

Figure 6 shows the topsoil temperature distributions during snow and snow free seasons. Similar to the discussion above, the snow free season shows large among-model discrepancies in topsoil temperature (Fig. 6b). The model inconsistency in snow free season is related to model representation of surface vegetation cover and litter/organic layers. 10 cm fixed moss cover in JSBACH and 10 cm litter layer in LPJ-GUESS brings similar amounts of insulation. At Samoylov, where strong vegetation cover is observed in the field, these models perform better for snow free season (Fig. 5c). However, at Bayelva, where vegetation effects are not that strong, 10 cm insulating layer proves to be too much and creates colder topsoil temperatures than observations (Figs. 5d and 6b). And for the bare Schilthorn site, even a thin layer of surface cover (2.5 cm litter layer) creates colder topsoil temperatures in LPJ-GUESS (Figs. 5b and 6b). These analyses support the need for such vegetation insulation in models during the snow free season, but the spatial heterogeneity of surface vegetation thickness remains an

TCD
8, 4959–5013, 2014

important source of uncertainty. A more detailed moss representation was used in Porada et al. (2013) and Rinke et al. (2008).

3.2 Soil thermal regime

Assessing soil thermal dynamics necessitates scrutinizing surface conditions as well as subsoil temperature dynamics. Being in contact with the atmosphere and surface cover, topsoil conditions show strong relations to seasonal surface processes and atmospheric changes. Despite their importance for the surface, above soil conditions are not enough to explain all the changes in subsoil temperature dynamics. Soil water and ice content, soil freezing and thawing, the characteristics and depth of the permafrost layer and its specific heat and water transfer mechanisms are especially important for cold regions' soil thermal regime. Therefore it is essential for models to capture deeper soil temperature dynamics together with the surface conditions.

Soil temperature evolutions of simulated soil layers are plotted for each model at each site in Figs. 7–10. Although Nuuk is a non-permafrost site, most of the models simulate subzero temperatures below 2–3 m at this site (Fig. 7). At the same time, those models show colder winter topsoil temperatures compared to observed values (Fig. 1a). Strong seasonal temperature changes are observed close to the surface, whereas temperature amplitudes are reduced in deeper layers and eventually a constant temperature is simulated at depths with zero annual amplitude (DZAA). At Nuuk, only ORCHIDEE and COUP simulate a true DZAA at around 2.5–3 m, while all other models show a minor temperature change even at their deepest layers. Together with the soil water/ice contents, simulating DZAA is partly related to the model soil depth and some models are limited by their shallow depth representations (Table 1).

At Schilthorn (Fig. 8), which is a high altitude permafrost site, JSBACH and JULES simulate above 0 °C temperatures (non-permafrost conditions) at deeper layers. In reality, there are almost isothermal conditions of about −0.7 °C between 7 m and at least 100 m depth at this site (PERMOS, 2013). This means a small temperature mismatch (on the order of 1 °C) can result in non-permafrost conditions. This kind of temperature bias would not affect the permafrost condition at colder sites (e.g. Samoylov). In addition, having low water and ice content, and a comparatively low albedo make the Schilthorn site very sensitive to interannual variations and make it more difficult for models to capture the soil thermal dynamics (Scherler et al., 2013). As previously mentioned, there is a contradictory bias in snow depth and topsoil temperature from ORCHIDEE and LPJ-GUESS simulations at Schilthorn (Fig. 4). Compared to other models (with snow representation), these models show colder subsurface temperatures at this site (Fig. 8), hence hindering heat penetration from the surface. As discussed in the previous section, a minimal surface littler layer (2.5 cm) in LPJ-GUESS contributes to the cooler Schilthorn soil temperatures in summer.

The simulated soil thermal regime at Samoylov reflects the colder climate at this site. All models show subzero temperatures below 1 m (Fig. 9). However, compared to other models, JULES and COUP show values much closer to 0 °C. As previously mentioned, subcritical snow conditions at this site amplify the soil temperature overestimation coming from snow depth bias (Fig. 4). Considering their better match during snow free season (Figs. 5c and 6b), the warmer temperatures in deeper layers of JULES and COUP can be attributed to snow conditions at this site. Additionally, these models include heat transfer via advection and conduction, while other models include just the latter. Together, these effects create warmer soil profiles.

At the high-Arctic Bayelva site, all models create permafrost conditions (Fig. 10). The JULES and COUP models again show warmer temperature profiles than the other models. As discussed above, these models include soil heat transfer by advection that is lacked by other models. In combination with that, COUP has a greater snow depth (Fig. 4), resulting in even warmer conditions than JULES. Such conditions demonstrate the importance of the combined effects of surface processes together with internal soil physics.

Apart from the permafrost conditions, the heat transfer rate also differs among models. Internal soil processes can impede the heat transfer and result in delayed warming or cooling of the deeper layers. JSBACH, ORCHIDEE, JULES and COUP show a more pronounced time lag of the heat/cold penetration into the soil, while HYBRID8 and LPJ-GUESS show either a very small lag or no lag at all (Figs. 7–10). This time lag is affected by the method of heat transfer, soil heat transfer parameters (soil heat capacity/conductivity), the amount of simulated phase change, vertical soil model resolution and internal model timestep. Given that all models use similar heat transfer methods including phase change (Table 1) and similar soil parameters (Table 3), the reason for the rapid warming/cooling at deeper layers of some models can be the lower amount of latent heat used/gained for the phase change, vertical resolution or model timestep. Even though the mineral (dry) heat transfer parameters are shared among models, they are modified afterwards due to the coupling of hydrology and thermal schemes. This leads to changes in the model heat conductivities depending on how much water/ice they simulate in that particular layer. Unfortunately, not all models output soil water/ice contents in a layered structure similar to soil temperature. This makes it difficult to assess the differences in modelled phase change and the consequent changes to soil heat transfer parameters. A better quantification of heat transfer rates would require a comparison of simulated water contents and soil heat conductivities among models, which is beyond the scope of this paper.

The soil thermal regime can also be investigated by studying the temperature profiles regarding minimum and maximum values (trumpet curves). Figure 11 shows the temperature envelopes of observed and simulated values at each site. The min. (max.) temperature curve represents the coldest (warmest) possible conditions for the soil thermal regime at a certain depth. The model biases in matching these curves are related to their topsoil temperature bias, soil heat transfer mechanism and bottom boundary conditions. As mentioned earlier, models without snow representation (e.g. HYBRID8) cannot match the min. curve in Fig. 11. However, snow depth bias (Fig. 4) cannot explain the min. curve mismatch for ORCHIDEE, COUP and LPJ-GUESS at Schilthorn (Fig. 11b). Furthermore, soil heat transfer methods or the bottom boundary conditions do not seem to play an important role for matching these soil temperature envelopes.

TCD
8, 4959–5013, 2014

3.3 Active layer thickness

As it is affected by the soil temperature profile, soil hydrology, surface insulation and atmospheric conditions, active layer thickness (ALT) is an integral measure of the soil thermal regime in permafrost soils. Figure 12 shows the yearly change of ALT and its relation to mean annual air temperature (MAAT) for the three permafrost sites. All models overestimate the ALT at Samoylov (Fig. 12b), but there is disagreement among models in overestimating or underestimating the ALT at Schilthorn (Fig. 12a) and Bayelva (Fig. 12c). Moreover, warmer atmospheric conditions result in deeper active layer depths as well as a larger range of modelled ALT values (Fig. 12d).

As discussed above, surface conditions (e.g. insulation) alone are not enough to explain the soil thermal regime, which affects ALT in turn. For Schilthorn, LPJ-GUESS generally shows shallower ALT values than other models; however it also shows the largest snow depth bias (Figs. 3 and 4). Normally, a larger snow depth leads to stronger insulation, so topsoil temperatures are expected to be warmer with corresponding increase in ALT values; however, this effect is overridden by other processes. The same holds true for ORCHIDEE results. If snow depth bias alone could explain the ALT difference, ORCHIDEE would have to show different values than HYBRID8, which completely lacks any snow representation. In addition to surface processes, subsoil temperatures and soil water and ice contents affect the ALT. At Schilthorn, COUP has high snow depth bias but still shows a very good match with ALT.

Overestimating snow depth (Fig. 4) seems to match with deeper ALT values in Samoylov (Fig. 12b). However, HYBRID8 does not have snow representation, yet it shows the deepest ALT values, which means snow insulation is not the reason for deeper ALT values in this model. Apart from not having any vegetation insulation, soil heat transfer is also much faster in HYBRID8 (see Sect. 3.2), which allows deeper penetration of summer warming into the soil column.

Surface conditions alone cannot describe the ALT bias in Bayelva either. LPJ-GUESS shows the lowest snow depth (Fig. 4) together with deepest ALT (Fig. 12c),

Discussion Paper | Discussion Paper | Discussion Paper | Discussion Paper |

TCD

8, 4959–5013, 2014

Site-level model intercomparison of high latitude and high altitude soil thermal dynamics

A. Ekici et al.

while JULES shows similar snow depth bias but the shallowest ALT values. As seen from Fig. 9, at this site LPJ-GUESS allows deeper heat penetration due to its higher heat transfer rate. So, apart from the snow conditions, a model's heat transfer rate is critical for predicting the ALT.

These results clearly show the risks of estimating ALT by topsoil temperatures alone. Many previous studies (Lunardini, 1981; Kudryatsevet al., 1974; Romanovsky and Osterkamp, 1997; Shiklomanov and Nelson, 1999; Stendel et al., 2007; Anisimov et al., 1997) used simple relationships connecting topsoil temperatures and ALT. By doing so, they attributed most of the ALT biases to insulation effects, which is mostly from snow processes in these regions. A good review of widely used analytical approximations and differences to numerical approaches is given by Riseborough et al. (2008). More recently, Koven et al. (2013) and Slater and Lawrence (2013) have highlighted large model uncertainties in estimating permafrost extent and ALT values with similar approaches relating topsoil temperatures and permafrost conditions in ESMs. However, other processes like the heat transfer scheme in the subsurface layers and resulting water and ice contents, are also important with regard to their impact on the soil temperature profile, and hence the ALT.

4 Conclusions

We have evaluated different land models' soil thermal dynamics against observations using a site-level approach. The analysis of the simulated soil thermal regime clearly reveals the importance of reliable surface insulation for topsoil temperature dynamics and of reliable soil heat transfer formulations for subsoil temperature and permafrost conditions at cold regions. Our findings include:

1. at high latitudes and altitudes, model snow depth bias explains most of the topsoil temperature biases.

TCD
8, 4959–5013, 2014

2. The snow insulation effect on topsoil temperature is amplified depending on the site snow conditions (sub-/supra-critical).

3. Snow depth underestimation in models always leads to a cold bias in topsoil temperature, whereas snow depth overestimation does not always lead to a warm bias in topsoil temperatures.

4. Surface vegetation cover and litter/organic layer insulation is important for topsoil temperatures in the snow free season, but models need more detailed representation of vegetation cover thickness.

5. There are significant differences in modelled soil heat transfer rates, which needs assessment of simulated soil water/ice contents and coupled heat transfer parameters.

6. Surface processes alone cannot explain the whole soil profile's thermal regime; subsoil conditions and model formulations affect the soil thermal dynamics.

7. Active layer thickness is related to both surface conditions and the soil thermal regime. ALT estimation by topsoil temperatures can bring large errors.

For permafrost and cold region related soil experiments, it is important for models to simulate the soil temperatures accurately, because permafrost extent, active layer thickness and the permafrost soil carbon processes are strongly related to soil temperatures. There is a major concern on how soil thermal state of these areas affect the ecosystem functions and what are the mechanisms (physical/biogeochemical) relating atmosphere, oceans and soils in cold regions. With the currently changing climate, the strengths of these couplings will be altered bringing more uncertainty for future projections.

In this paper, we have shown the current state of some land models in capturing surface/subsurface temperatures at different cold region landscapes. It is evident that

TCD
8, 4959–5013, 2014

there is much uncertainty especially for above surface processes as well as soil internal physics of model formulations. To achieve better confidence in future simulations, model developments should include better insulation processes (for snow: compaction, metamorphism, depth hoar, wind drift; for moss: dynamic thickness and wetness) and more detailed evaluation of their soil heat transfer rates with observed data (comparing simulated ice contents and soil heat conductivities).

Appendix A: Model layering schemes and depths of soil temperature observations

Exact depths of each soil layer used in model formulations:

JSBACH:	0.065, 0.254, 0.913, 2.902, 5.7 m
ORCHIDEE:	0.04, 0.05, 0.06, 0.07, 0.08, 0.1, 0.11, 0.14, 0.16, 0.19, 0.22, 0.27, 0.31, 0.37, 0.43, 0.52, 0.61, 0.72, 0.84, 1.00, 1.17, 1.39, 1.64, 1.93, 2.28, 2.69, 3.17, 3.75, 4.42, 5.22, 6.16, 7.27 m
JULES:	0.1, 0.25, 0.65, 2.0 m
COUP:	different for each site
Nuuk:	0.01 m intervals until 0.36 m, then 0.1 m intervals until 2 m and then 0.5 m intervals until 6 m
Schilthorn:	0.05 m then 0.1 m intervals until 7 m, and then 0.5 m intervals until 13 m
Samoylov:	0.05 m then 0.1 m intervals until 5 m, and then 0.5 m intervals until 8 m
Bayelva:	0.01 m intervals until 0.3 m, then 0.1 m intervals until 1 m and then 0.5 m intervals until 6 m
HYBRID8:	different for each site
Nuuk:	0.07, 0.29, 1.50, 5.00 m

TCD
8, 4959–5013, 2014

Title Page
Abstract | Introduction
Conclusions | References
Tables | Figures
Back | Close
Full Screen / Esc
Printer-friendly Version
Interactive Discussion

Schilthorn: 0.07, 0.30, 1.50, 5.23 m
Samoylov: 0.07, 0.30, 1.50, 6.13 m
Bayelva: 0.07, 0.23, 1.50, 5.00 m
LPJ-GUESS: 0.1 m intervals until 2 m (additional padding layer of 48 m depth)

Depts of soil temperature observations for each site:

NUUK: 0.01, 0.05, 0.10, 0.30 m
SCHILTHORN: 0.20, 0.40, 0.80, 1.20, 1.60, 2.00, 2.50, 3.00, 3.50, 4.00, 5.00, 7.00, 9.00, 10.00 m
SAMOYLOV: 0.02, 0.06, 0.11, 0.16, 0.21, 0.27, 0.33, 0.38, 0.51, 0.61, 0.71 m
BAYELVA: 0.06, 0.24, 0.40, 0.62, 0.76, 0.99, 1.12 m

Acknowledgements. The research leading to these results has received funding from the European Community's Seventh Framework Programme (FP7 2007–2013) under grant agreement no. 238366. Authors also acknowledge the BMBF project CarboPerm for the funding. Nuuk site monitoring data for this paper were provided by the GeoBasis program run by Department of Geography, University of Copenhagen and Department of Bioscience, Aarhus University, Denmark. The program is part of the Greenland Environmental Monitoring (GEM) Program (www.g-e-m.dk) and financed by the Danish Environmental Protection Agency, Danish Ministry of the Environment. We would like to acknowledge a grant of the Swiss National Science Foundation (Sinergia TEMPS project, no. CRSII2 136279) for the COUP model intercomparison, as well as the Swiss PERMOS network for the Schilthorn data provided. Authors also acknowledge financial support from DEFROST, a Nordic Centre of Excellence (NCoE) under the Nordic Top-level Research Initiative (TRI), and the Lund University Centre for Studies of Carbon Cycle and Climate Interactions (LUCCI). E. Burke was supported by the Joint UK DECC/Defra Met Office Hadley Centre Climate Programme (GA01101) and the European Union Seventh Framework Programme (FP7/2007–2013) under

TCD
8, 4959–5013, 2014

grant agreement no. 282700, which also provided the Samoylov site data.

The service charges for this open access publication have been covered by the Max Planck Society.

References

Abnizova, A., Siemens, J., Langer, M., and Boike, J.: Small ponds with major impact: the relevance of ponds and lakes in permafrost landscapes to carbon dioxide emissions, Global Biogeochem. Cy., 26, GB2041, doi:10.1029/2011GB004237, 2012.

Abramopoulos, F., Rosenzweig, C., and Choudhury, B.: Improved ground hydrology calculations for global climate models (GCMs): soil water movement and evapotranspiration, J. Climate, 1, 921–941, doi:10.1175/1520-0442(1988)001<0921:IGHCFG>2.0.CO;2, 1988.

ACIA: Arctic Climate Impact Assessment, Cambridge University Press, New York, USA, 1042 pp., 2005.

Anderson, D. M., Tice, A. R., and McKim, H. L.: The unfrozen water and the apparent specific heat capacity of frozen soils, in: Permafrost: North American Contributions to the Second International Conference, Yakutsk, Siberia, USSR, National Academy of Sciences, Washington, DC, 13–18 July 1973, 20418, 289–295, 1973.

Anisimov, O. A. and Nelson, F. E.: Permafrost zonation and climate change in the Northern Hemisphere: results from transient general circulation models, Climatic Change, 35, 241–258, doi:10.1023/A:1005315409698, 1997.

Beer, C., Weber, U., Tomelleri, E., Carvalhais, N., Mahecha, M., and Reichstein, M.: Harmonized European long-term climate data for assessing the effect of changing temporal variability on land–atmosphere CO_2 fluxes, J. Climate, 27, 4815–4834, doi:10.1175/JCLI-D-13-00543.1, 2014.

Best, M. J., Pryor, M., Clark, D. B., Rooney, G. G., Essery, R.L. H., Ménard, C. B., Edwards, J. M., Hendry, M. A., Porson, A., Gedney, N., Mercado, L. M., Sitch, S., Blyth, E., Boucher, O., Cox, P. M., Grimmond, C. S. B., and Harding, R. J.: The Joint UK Land Environment Simulator (JULES), model description – Part 1: Energy and water fluxes, Geosci. Model Dev., 4, 677–699, doi:10.5194/gmd-4-677-2011, 2011.

Boike, J., Roth, K., and Ippisch, O.: Seasonal snow cover on frozen ground: energy balance calculations of a permafrost site near Ny-Ålesund, Spitsbergen, J. Geophys. Res.-Atmos., 108, 1–11, D28163, doi:10.1029/2001JD000939, 2003.

Boike, J., Ippisch, O., Overduin, P. P., Hagedorn, B., and Roth, K.: Water, heat and solute dynamics of a mud boil, Spitsbergen, Geomorphology, 95, 61–73, doi:10.1016/j.geomorph.2006.07.033, 2007.

Boike, J., Wille, C., and Abnizova, A.: Climatology and summer energy and water balance of polygonal tundra in the Lena River Delta, Siberia, J. Geophys. Res., 113, G03025, doi:10.1029/2007JG000540, 2008.

Boike, J., Kattenstroth, B., Abramova, K., Bornemann, N., Chetverova, A., Fedorova, I., Fröb, K., Grigoriev, M., Grüber, M., Kutzbach, L., Langer, M., Minke, M., Muster, S., Piel, K., Pfeiffer, E.-M., Stoof, G., Westermann, S., Wischnewski, K., Wille, C., and Hubberten, H.-W.: Baseline characteristics of climate, permafrost and land cover from a new permafrost observatory in the Lena River Delta, Siberia (1998–2011), Biogeosciences, 10, 2105–2128, doi:10.5194/bg-10-2105-2013, 2013.

Burke, E. J., Dankers, R., Jones, C. D., and Wiltshire, A. J.: A retrospective analysis of pan Arctic permafrost using the JULES land surface model, Clim. Dynam., 41, 1025–1038, 2013.

Clark, D. B., Mercado, L. M., Sitch, S., Jones, C. D., Gedney, N., Best, M. J., Pryor, M., Rooney, G. G., Essery, R. L. H., Blyth, E., Boucher, O., Harding, R. J., Huntingford, C., and Cox, P. M.: The Joint UK Land Environment Simulator (JULES), model description – Part 2: Carbon fluxes and vegetation dynamics, Geosci. Model Dev., 4, 701–722, doi:10.5194/gmd-4-701-2011, 2011.

Cox, P. M., Betts, R. A., Bunton, C. B., Essery, R. L. H., Rowntree, P. R., and Smith, J.: The impact of new land surface physics on the GCM simulation of climate and climate sensitivity, Clim. Dynam., 15, 183–203, 1999.

Dankers, R., Burke, E. J., and Price, J.: Simulation of permafrost and seasonal thaw depth in the JULES land surface scheme, The Cryosphere, 5, 773–790, doi:10.5194/tc-5-773-2011, 2011.

Ekici, A., Beer, C., Hagemann, S., Boike, J., Langer, M., and Hauck, C.: Simulating high-latitude permafrost regions by the JSBACH terrestrial ecosystem model, Geosci. Model Dev., 7, 631–647, doi:10.5194/gmd-7-631-2014, 2014.

Engelhardt, M., Hauck, C., and Salzmann, N.: Influence of atmospheric forcing parameters on modelled mountain permafrost evolution, Meteorol. Z., 19, 491–500, 2010.

FAO, IIASA, ISRIC, ISS-CAS, and JRC: Harmonized World Soil Database (version 1.1), FAO, Rome, Italy and IIASA, Laxenburg, Austria, 2009.
Fiddes, J., Endrizzi, S., and Gruber, S.: Large area land surface simulations in heterogeneous terrain driven by global datasets: application to mountain permafrost, The Cryosphere Discuss., 7, 5853–5887, doi:10.5194/tcd-7-5853-2013, 2013.
Friend, A. D.: Terrestrial plant production and climate change, J. Exp. Bot., 61, 1293–1309, doi:10.1093/jxb/erq019, 2010.
Friend, A. D. and Kiang, N. Y.: Land-surface model development for the GISS GCM: effects of improved canopy physiology on simulated climate, J. Climate, 18, 2883–2902, doi:10.1175/JCLI3425.1, 2005.
Friend, A. D., Geider, R. J., Behrenfeld, M. J., and Still, C. J.: Photosynthesis in global-scale models, in: Photosynthesis in Silico: Understanding Complexity from Molecules to Ecosystems, Springer Series "Advances in Photosynthesis and Respiration", Vol 29, edited by: Laisk, A., Nedbal, L., and Govindjee, Springer, Dordrecht, the Netherlands, 465–497, 2009.
Gerten, D., Schaphoff, S., Haberlandt, U., Lucht, W., and Sitch, S.: Terrestrial vegetation and water balance – hydrological evaluation of a dynamic global vegetation model, J. Hydrol., 286, 249–270, 2004.
Gornall, J. L., Jonsdottir, I. S., Woodin, S. J., and Van der Wal, R.: Arctic mosses govern below-ground environment and ecosystem processes, Oecologia, 153, 931–941, doi:10.1007/s00442-007-0785-0, 2007.
Gouttevin, I., Krinner, G., Ciais, P., Polcher, J., and Legout, C.: Multi-scale validation of a new soil freezing scheme for a land-surface model with physically-based hydrology, The Cryosphere, 6, 407–430, doi:10.5194/tc-6-407-2012, 2012a.
Gouttevin, I., Menegoz, M., Domine, F., Krinner, G., Koven, C. D., Ciais, P., Tarnocai, C., and Boike, J.: How the insulating properties of snow affect soil carbon distribution in the continental pan-Arctic area, J. Geophys. Res., 117, G02020, doi:10.1029/2011JG001916, 2012b.
Gubler, S., Endrizzi, S., Gruber, S., and Purves, R. S.: Sensitivities and uncertainties of modeled ground temperatures in mountain environments, Geosci. Model Dev., 6, 1319–1336, doi:10.5194/gmd-6-1319-2013, 2013.
Gustafsson, D., Stähli, M., and Jansson, P.-E.: The surface energy balance of a snow cover: comparing measurements to two different simulation models, Theor. Appl. Climatol., 70, 81–96, 2001.

TCD
8, 4959–5013, 2014

Site-level model intercomparison of high latitude and high altitude soil thermal dynamics

A. Ekici et al.

Harlan, R. L.: Analysis of coupled heat-fluid transport in partially frozen soil, Water Resour. Res., 9, 1314–1323, 1973.

Harris, C., Arenson, L., Christiansen, H., Etzelmüller, B., Frauenfelder, R., Gruber, S., Haeberli, W., Hauck, C., Hoelzle, M., Humlum, O., Isaksen, K., Kääb, A., Kern-Lütschg, M., Lehning, M., Matsuoka, N., Murton, J., Nötzli, J., Phillips, M., Ross, N., Seppälä, M., Springman, S., and Vonder Mühll, D.: Permafrost and climate in Europe: monitoring and modelling thermal, geomorphological and geotechnical responses, Earth-Sci. Rev., 92, 117–171, 2009.

Hauck, C.: Frozen ground monitoring using DC resistivity tomography, Geophys. Res. Lett., 29, 2016, doi:10.1029/2002GL014995, 2002.

Helbig, M., Boike, J., Langer, M., Schreiber, P., Runkle, B. R., and Kutzbach, L.: Spatial and seasonal variability of polygonal tundra water balance: Lena River Delta, northern Siberia (Russia), Hydrogeol. J., 21, 133–147, 2013.

Hilbich, C., Hauck, C., Hoelzle, M., Scherler, M., Schudel, L., Völksch, I., Vonder Mühll, D., and Mäusbacher, R.: Monitoring mountain permafrost evolution using electrical resistivity tomography: a 7 year study of seasonal, annual, and long-term variations at Schilthorn, Swiss Alps, J. Geophys. Res., 113, F01S90, doi:10.1029/2007JF000799, 2008.

Hilbich, C., Fuss, C., and Hauck, C.: Automated time-lapse ERT for improved process analysis and monitoring of frozen ground, Permafrost Periglac., 22, 306–319, doi:10.1002/ppp.732, 2011.

Hoelzle, M. and Gruber, S.: Borehole and ground surface temperatures and their relationship to meteorological conditions in the Swiss Alps, in: Proceedings Ninth International Conference on Permafrost, 29 June–3 July, Fairbanks, Alaska, vol. 1, edited by: Kane, D. L. and Hinkel, K. M., Institute of Northern Engineering, University of Alaska Fairbanks, 723–728, 2008.

Hollesen, J., Elberling, B., and Jansson, P. E.: Future active layer dynamics and carbon dioxide production from thawing permafrost layers in Northeast Greenland, Glob. Change Biol., 17, 911–926, doi:10.1111/j.1365-2486.2010.02256.x, 2011.

IPCC AR5: Summary for Policymakers, Climate Change 2013. The Physical Science Basis, Contribution of Working Group I to the Fifth Assessment Report of the Intergovernmental Panel on Climate Change, edited by: Stocker, T. F., Qin, D., Plattner, G.-K., Tignor, M., Allen, S. K., Boschung, J., Nauels, A., Xia, Y., Bex, V., and Midgley, P. M., Cambridge University Press, Cambridge, UK and New York, NY, USA, 2013.

Jansson, P. E.: CoupModel: model use, calibration, and validation, T. ASABE, 55, 1335–1344, 2012.
Jansson, P.-E. and Karlberg, L.: Coupled Heat and Mass Transfer Model for Soil–Plant–Atmosphere Systems, Royal Institute of Technology, Dept of Civil and Environmental Engineering, Stockholm, available at: http://www.lwr.kth.se/Vara%20Datorprogram/CoupModel/index.htm (last access: 17 September 2013), 2011.
Jensen, L. M. and Rasch, M.: Nuuk Ecological Research Operations, 2nd Annual Report, 2008, Roskilde, National Environment Research Institute, Aarhus University, Denmark, 80 pp., 2009.
Jensen, L. M. and Rasch, M.: Nuuk Ecological Research Operations, 3rd Annual Report, 2009, Roskilde, National Environment Research Institute, Aarhus University, Denmark, 80 pp., 2010.
Jungclaus, J. H., Fischer, N., Haak, H., Lohmann, K., Marotzke, J., Matei, D., Mikolajewicz, U., Notz, D., and von Storch, J. S.: Characteristics of the ocean simulations in MPIOM, the ocean component of the MPI-Earth System Model, J. Adv. Model. Earth Syst., 5, 422–446, doi:10.1002/jame.20023, 2013.
Koven, C. D., Ringeval, B., Friedlingstein, P., Ciais, P., Cadule, P., Khvorostyanov, D., Krinner, G., and Tarnocai, C.: Permafrost carbon-climate feedbacks accelerate global warming, P. Natl. Acad. Sci. USA, 108, 36, 14769–14774, doi:10.1073/pnas.1103910108, 2011.
Koven, C. D., William, J. R., and Alex, S.: Analysis of permafrost thermal dynamics and response to climate change in the CMIP5 earth system models, J. Climate, 26, 1877–1900, doi:10.1175/JCLI-D-12-00228.1, 2013.
Krinner, G., Viovy, N., de Noblet-Ducoudré, N., Ogé, J., Polcher, J., Friedlingstein, P., Ciais, P., Sitch, S., and Prentice, I. C.: A dynamic global vegetation model for studies of the coupled atmosphere–biosphere system, Global Biogeochem. Cy., 19, GB1015, doi:10.1029/2003GB002199, 2005.
Kudryavtsev, V. A., Garagulya, L. S., Kondrat'yeva, K. A., and Melamed, V. G.: Fundamentals of Frost Forecasting in Geological Engineering Investigations, Cold Regions Reseach and Engineering Laboratory, Hanover, NH, 1974.
Kutzbach, L., Wille, C., and Pfeiffer, E.-M.: The exchange of carbon dioxide between wet arctic tundra and the atmosphere at the Lena River Delta, Northern Siberia, Biogeosciences, 4, 869–890, doi:10.5194/bg-4-869-2007, 2007.

Langer, M., Westermann, S., Heikenfeld, M., Dorn, W., and Boike, J.: Satellite-based modeling of permafrost temperatures in a tundra lowland landscape, Remote Sens. Environ., 135, 12–24, doi:10.1016/j.rse.2013.03.011, 2013.
Larsen, P. H., Goldsmith, S., Smith, O., Wilson, M. L., Strzepek, K., Chinowsky, P., and Saylor, B.: Estimating future costs for Alaska public infrastructure at risk from climate change, Global Environ. Chang., 18, 442–457, doi:10.1016/j.gloenvcha.2008.03.005, 2008.
Lawrence, D. M., Slater, A. G., Romanovsky, V. E., and Nicolsky, D. J.: Sensitivity of a model projection of near-surface permafrost degradation to soil column depth and representation of soil organic matter, J. Geophys. Res., 113, 1–14, 2008.
Lunardini, V. J.: Heat Transfer in Cold Climates, Van Nostrand Reinhold, New York, 1981.
Lundin, L. C.: Hydraulic properties in an operational model of frozen soil, J. Hydrol., 118, 289–310, 1990.
Lüers, J., Westermann, S., Piel, K., and Boike, J.: Annual CO_2 budget and seasonal CO_2 exchange signals at a High Arctic permafrost site on Spitsbergen, Svalbard archipelago, Biogeosciences Discuss., 11, 1535–1559, doi:10.5194/bgd-11-1535-2014, 2014.
Mahecha, M. D., Reichstein, M., Jung, M., Seneviratne, S. I., Zaehle, S., Beer, C., Braakhekke, M. C., Carvalhais, N., Lange, H., Le Maire, G., and Moors, E.: Comparing observations and process-based simulations of biosphere–atmosphere exchanges on multiple timescales, J. Geophys. Res., 115, G02003, doi:10.1029/2009JG001016, 2010.
Marmy, A., Salzmann, N., Scherler, M., and Hauck, C.: Permafrost model sensitivity to seasonal climatic changes and extreme events in mountainous regions, Environ. Res. Lett., 8, 035048, doi:10.1088/1748-9326/8/3/035048, 2013.
Maturilli, M., Herber, A., and König-Langlo, G.: Climatology and time series of surface meteorology in Ny-Ålesund, Svalbard, Earth Syst. Sci. Data, 5, 155–163, doi:10.5194/essd-5-155-2013, 2013.
McGuire, A. D., Christensen, T. R., Hayes, D., Heroult, A., Euskirchen, E., Kimball, J. S., Koven, C., Lafleur, P., Miller, P. A., Oechel, W., Peylin, P., Williams, M., and Yi, Y.: An assessment of the carbon balance of Arctic tundra: comparisons among observations, process models, and atmospheric inversions, Biogeosciences, 9, 3185–3204, doi:10.5194/bg-9-3185-2012, 2012.
Miller, P. A. and Smith, B.: Modeling tundra vegetation response to recent Arctic warming, AMBIO, 41, 281–291, 2012.

Muster, S., Langer, M., Heim, B., Westermann, S., and Boike, J.: Subpixel heterogeneity of ice-wedge polygonal tundra: a multi-scale analysis of land cover and evapotranspiration in the Lena River Delta, Siberia, Tellus B, 64, 17301, doi:10.3402/tellusb.v64i0.17301, 2012.

PERMOS: Permafrost in Switzerland 2008/2009 and 2009/2010, edited by: Noetzli, J., Glaciological Report (Permafrost) No. 10/11 of the Cryospheric Commission of the Swiss Academy of Sciences (SCNAT), Zurich, Switzerland, 2013.

Porada, P., Weber, B., Elbert, W., Pöschl, U., and Kleidon, A.: Estimating global carbon uptake by lichens and bryophytes with a process-based model, Biogeosciences, 10, 6989–7033, doi:10.5194/bg-10-6989-2013, 2013.

Rinke, A., Kuhry, P., and Dethloff, K.: Importance of a soil organic layer for Arctic climate: a sensitivity study with an Arctic RCM, Geophys. Res. Lett., 35, L13709, doi:10.1029/2008GL034052, 2008.

Riseborough, D., Shiklomanov, N., Etzelmuller, B., Gruber, S., and Marchenko, S.: Recent advances in permafrost modelling, Permafrost Periglac., 19, 137–156, 2008.

Romanovsky, V. E. and Osterkamp, T. E.: Thawing of the active layer on the coastal plain of the Alaskan Arctic, Permafrost Periglac., 8, 1–22, doi:10.1002/(SICI)1099-1530(199701)8:1<1::AID-PPP243>3.0.CO;2-U, 1997.

Romanovsky, V. E., Smith, S. L., and Christiansen, H. H.: Permafrost thermal state in the polar Northern Hemisphere during the international polar year 2007–2009: a synthesis, Permafrost Periglac., 21, 106–116, 2010.

Rosenzweig, C. and Abramopoulos, F.: Land–surface model development for the GISS GCM, J. Climate, 10, 2040–2054, doi:10.1175/1520-0442(1997)010<2040:LSMDFT>2.0.CO;2,1997.

Roth, K. and Boike, J.: Quantifying the thermal dynamics of a permafrost site near Ny-Ålesund, Svalbard, Water Resour. Res., 37, 2901–2914, doi:10.1029/2000WR000163, 2001.

Schaefer, K., Zhang, T., Slater, A. G., Lu, L., Etringer, A., and Baker, I.: Improving simulated soil temperatures and soil freeze/thaw at high-latitude regions in the Simple Biosphere/Carnegie–Ames–Stanford Approach model, J. Geophys. Res., 114, F02021, doi:10.1029/2008JF001125, 2009.

Scherler, M., Hauck, C., Hoelzle, M., Stähli, M., and Völksch, I.: Meltwater infiltration into the frozen active layer at an alpine permafrost site, Permafrost Periglac., 21, 325–334, doi:10.1002/ppp.694, 2010.

Scherler, M., Hauck, C., Hoelzle, M., and Salzmann, N.: Modeled sensitivity of two alpine permafrost sites to RCM-based climate scenarios, J. Geophys. Res.-Earth, 118, 780–794, doi:10.1002/jgrf.20069, doi:10.1002/jgrf.20069, 2013.

Schmidt, G. A., Ruedy, R., Hansen, J. E., Aleinov, I., Bell, N., Bauer, M., Bauer, S., Cairns, B., Canuto, V., Cheng, Y., Del Genio, A., Faluvegi, G, Friend, A. D., Hall, T. M., Hu, Y., Kelley, M., Kiang, N. Y., Koch, D., Lacis, A. A., Lerner, J., Lo, K. K., Miller, R. L., Nazarenko, L., Oinas, V., Perlwitz, Ja., Perlwitz, Ju., Rind, D., Romanou, A., Russell, G. L., Sato, MKi., Shindell, D. T., Stone, P. H., Sun, S., Tausnev, N., Thresher, D., and Yao, M. S.: Present day atmospheric simulations using GISS ModelE: comparison to in-situ, satellite and reanalysis data, J. Climate, 19, 153–192, 2006.

Schuur, E. A. G., Bockheim, J., Canadell, J. G., Euskirchen, E., Field, C. B., Goryachkin, S. V., Hagemann, S., Kuhry, P., Lafleur, P. M., Lee, H., Mazhitova, G., Nelson, F. E., Rinke, A., Romanovsky, V. E., Shiklomanov, N., Tarnocai, C., Venevsky. S., Vogel, J. G., and Zimov, S. A.: Vulnerability of permafrost carbon to climate change: implications for the global carbon cycle, BioScience, 58, 701–714, 2008.

Serreze, M., Walsh, J., Chapin, F., Osterkamp, T., Dyurgerov, M., Romanovsky, V., Oechel, W., Morison, J., Zhang, T., and Barry, R.: Observational evidence of recent change in the northern highlatitude environment, Climatic Change, 46, 159–207, 2000.

Shiklomanov, N. I. and Nelson, F. E.: Analytic representation of the active layer thickness field, Kuparuk River Basin, Alaska, Ecol. Model., 123, 105–125, doi:10.1016/S0304-3800(99)00127-1, 1999.

Sitch, S., Smith, B., Prentice, I. C., Arneth, A., Bondeau, A., Cramer, W., Kaplan, J. O., Levis, S., Lucht, W., Sykes, M. T., Thonicke, K., and Venevsky, S.: Evaluation of ecosystem dynamics, plant geography and terrestrial carbon cycling in the LPJ dynamic global vegetation model, Glob. Change Biol., 9, 161–185, 2003.

Slater, A. G. and Lawrence, D. M.: Diagnosing present and future permafrost from climate models, J. Climate, 26, 5608–5623, doi:10.1175/JCLI-D-12-00341.1, 2013.

Smith, B., Prentice, I. C., and Sykes, M. T.: Representation of vegetation dynamics in the modelling of terrestrial ecosystems: comparing two contrasting approaches within European climate space, Global Ecol. Biogeogr., 10, 621–637, doi:10.1046/j.1466-822X.2001.t01-1-00256.x, 2001.

Soudzilovskaia, N. A., van Bodegom, P. M., and Cornelissen, J. H. C.: Dominant bryophyte control over high-latitude soil temperature fluctuations predicted by heat transfer traits, field mois-

ture regime and laws of thermal insulation, Funct. Ecol., 27, 1442–1454, doi:10.1111/1365-2435.12127, 2013.
Stendel, M., Romanovsky, V. E., Christensen, J. H., and Sazonova, T.: Using dynamical downscaling to close the gap between global change scenarios and local permafrost dynamics, Global Planet. Change, 56, 203–214, doi:10.1016/j.gloplacha.2006.07.014, 2007.
Stevens, B., Giorgetta, M., Esch, M., Mauritsen, T., Crueger, T., Rast, S., Salzmann, M., Schmidt, H., Bader, J., Block, K., Brokopf, R., Fast, I., Kinne, S., Kornblueh, L., Lohmann, U., Pincus, R., Reichler, T., and Roeckner, E.: The atmospheric component of the MPI-M Earth System Model: ECHAM6, J. Adv. Model. Earth Syst., 5, 146–172, doi:10.1002/jame.20015, 2012.
Taylor, K. E., Stouffer, R. J., and Meehl, G. A.: A Summary of the CMIP5 Experiment Design, PCMDI Tech. Rep., 33 pp., available at: http://cmip-pcmdi.llnl.gov/cmip5/docs/Taylor_CMIP5_design.pdf (last access: 12 November 2013), 2009.
Vonder Mühll, D., Hauck, C., and Lehmann, F.: Verification of geophysical models in Alpine permafrost using borehole information, Ann. Glaciol., 31, 300–306, 2000.
Wang, T., Ottle, C., Boone, A., Ciais, P., Brun, E., Morin, S., Krinner, G., Piao, S., and Peng, S.: Evaluation of an improved intermediate complexity snow scheme in the ORCHIDEE land surface model, J. Geophys. Res.-Atmos., 118, 6064–6079, doi:10.1002/jgrd.50395, 2013.
Wania, R., Ross, I., and Prentice, I. C.: Integrating peatlands and permafrost into a dynamic global vegetation model: 1. Evaluation and sensitivity of physical land surface processes, Global Biogeochem. Cy., 23, GB3014, doi:10.1029/2008GB003412, 2009a.
Wania, R., Ross, I., and Prentice, I. C.: Integrating peatlands and permafrost into a dynamic global vegetation model: 2. Evaluation and sensitivity of vegetation and carbon cycle processes, Global Biogeochem. Cy., 23, GB3015, doi:10.1029/2008GB003413, 2009b.
Wania, R., Ross, I., and Prentice, I. C.: Implementation and evaluation of a new methane model within a dynamic global vegetation model: LPJ-WHyMe v1.3.1, Geosci. Model Dev., 3, 565–584, doi:10.5194/gmd-3-565-2010, 2010.
Weedon, G., Gomes, S., Viterbo, P., Österle, H., Adam, J., Bellouin, N., Boucher, O., and Best, M.: The WATCH Forcing Data 1958–2001: A Meteorological Forcing Dataset for Land Surface and Hydrological Models, WATCH Tech. Rep. 22, 41 pp., available at: http://www.eu-watch.org/publications/technical-reports (last access: 20 June 2013), 2010.

TCD
8, 4959–5013, 2014

Site-level model intercomparison of high latitude and high altitude soil thermal dynamics

A. Ekici et al.

Westermann, S., Lüers, J., Langer, M., Piel, K., and Boike, J.: The annual surface energy budget of a high-arctic permafrost site on Svalbard, Norway, The Cryosphere, 3, 245–263, doi:10.5194/tc-3-245-2009, 2009.
Westermann, S., Wollschläger, U., and Boike, J.: Monitoring of active layer dynamics at a permafrost site on Svalbard using multi-channel ground-penetrating radar, The Cryosphere, 4, 475–487, doi:10.5194/tc-4-475-2010, 2010.
Westermann, S., Langer, M., and Boike, J.: Spatial and temporal variations of summer surface temperatures of high-arctic tundra on Svalbard – implications for MODIS LST based permafrost monitoring, Remote Sens. Environ., 115, 908–922, doi:10.1016/j.rse.2010.11.018, 2011.
Wolf, A., Callaghan, T., and Larson, K.: Future changes in vegetation and ecosystem function of the Barents Region, Climatic Change, 87, 51–73, 2008.
Zhang, T.: Influence of the seasonal snow cover on the ground thermal regime: an overview, Rev. Geophys., 43, RG4002, doi:10.1029/2004RG000157, 2005.
Zhang, W., Miller, P. A., Smith, B., Wania, R., Koenigk, T., and Döscher, R.: Tundra shrubification and tree-line advance amplify arctic climate warming: results from an individual-based dynamic vegetation model, Environ. Res. Lett., 8, 034023, doi:10.1088/1748-9326/8/3/034023, 2013.

Table 1. Model details related to soil heat transfer.

	JSBACH	ORCHIDEE	JULES	COUP	HYBDRID8	LPJ-GUESS
Soil freezing	Yes	Yes	Yes	Yes	Yes	Yes
Soil heat transfer method	Conduction	Conduction	Conduction Advection	Conduction Advection	Conduction Advection	Conduction
Dynamic soil heat transfer parameters	Yes	Yes	Yes	Yes	Yes	Yes
Soil depth	10 m	47 m	3 m	Variable (> 5 m)	Variable (> 5 m)	2 m
Bottom boundary condition	Zero heat flux	Geothermal heat flux (0.057 $W m^{-2}$)	Zero heat flux	Geothermal heat flux (0.011 $W m^{-2}$)	Zero heat flux	Zero heat flux
Snow layering	5 layers	3 layers	3 layers	1 layer	No snow representation	1 layer
Dynamic snow heat transfer parameters	No	Yes	Yes	Yes	–	Yes (only heat capacity)
Insulating moss/litter cover	10 cm moss layer	–	–	–	–	Site-specific litter layer
Model timestep	30 min	30 min	30 min	30 min	30 min	1 day

TCD
8, 4959–5013, 2014

Table 2. Site details.

	NUUK	SCHILTHORN	SAMOYLOV	BAYELVA
Latitude	64.13° N	46.56° N	72.4° N	78.91° N
Longitude	51.37° W	7.08° E	126.5° E	11.95° E
Mean annual air temperature	−1.3 °C	−2.7 °C	−13 °C	−4.4 °C
Mean annual ground temperature	3.2 °C	−0.45 °C	−10 °C	−2/−3 °C
Annual precipitation	900 mm	1963 mm	200 mm	400 mm
Avg. length of snow cover	7 months	9.5 months	9 months	9 months
Vegetation cover	Tundra	Barren	Tundra	Tundra

TCD
8, 4959–5013, 2014

TCD
8, 4959–5013, 2014

Table 3. Details of driving data preparation for site simulations.

		NUUK	SCHILTHORN	SAMOYLOV	BAYELVA
ATMOSPHERIC FORCING VARIABLES	Air temperature	In situ	In situ	In situ	In situ
	Precipitation	In situ	In situ	In situ (snow season from WATCH)	In situ
	Air pressure	In situ	WATCH	WATCH	In situ
	Atm. humidity	In situ	In situ	In situ	In situ
	Incoming longwave radiation	In situ	In situ	In situ	WATCH
	Incoming shortwave radiation	In situ	In situ	WATCH	In situ
	Net radiation	In situ	–	In situ	–
	Wind speed	In situ	In situ	In situ	In situ
	Wind direction	In situ	–	In situ	–
	Time period	26 Jun 2008–31 Dec 2011	1 Oct 1999–30 Sep 2008	14 Jul 2003–11 Oct 2005	1 Jan 1998–31 Dec 2009
STATIC SOIL PARAMETERS	Soil porosity	46 %	50 %	60 %	41 %
	Soil field capacity	36 %	44 %	31 %	22 %
	Mineral soil depth	36 cm	710 cm	800 cm	30 cm
	Dry soil heat capacity	2.213×10^6 ($J\,m^{-3}\,K^{-1}$)	2.203×10^6 ($J\,m^{-3}\,K^{-1}$)	2.1×10^6 ($J\,m^{-3}\,K^{-1}$)	2.165×10^6 ($J\,m^{-3}\,K^{-1}$)
	Dry soil heat conductivity	6.84 ($W\,m^{-1}\,K^{-1}$)	7.06 ($W\,m^{-1}\,K^{-1}$)	5.77 ($W\,m^{-1}\,K^{-1}$)	7.93 ($W\,m^{-1}\,K^{-1}$)
	Sat. hydraulic conductivity	2.42×10^{-6} (ms^{-1})	4.19×10^{-6} (ms^{-1})	2.84×10^{-6} (ms^{-1})	7.11×10^{-6} (ms^{-1})
	Saturated moisture potential	0.00519 (m)	0.2703 (m)	0.28 (m)	0.1318 (m)

Table 4. Details of model spin up procedures.

	JSBACH	ORCHIDEE	JULES	COUP	HYBRID8	LPJ-GUESS
Spin-up data	Observed climate	Observed climate	Observed climate	Observed climate	Observed climate	WATCH* data
Spin-up duration	50 years	10 000 years	50 years	10 years	50 years	500 years

* 500 years forced with monthly WATCH reanalysis data from the 1901–1930 period, followed by daily WATCH forcing from 1901–until YYYY-MM-DD, then daily site-data.

TCD
8, 4959–5013, 2014

Table A1. Selected depths of observed and modeled soil temperatures referred as "topsoil temperature" in Figs. 1, 2, and 4–6.

	Nuuk	Schilthorn	Samoylov	Bayelva
OBSERVATION	5 cm	20 cm	6 cm	6 cm
JSBACH	3.25 cm	18.5 cm	3.25 cm	3.25 cm
ORCHIDEE	6.5 cm	18.5 cm	6.5 cm	6.5 cm
JULES	5 cm	22.5 cm	5 cm	5 cm
COUP	5.5 cm	20 cm	2.5 cm	5.5 cm
HYBRID8	3.5 cm	22 cm	3.5 cm	3.5 cm
LPJ-GUESS	5 cm	25 cm	5 cm	5 cm

TCD
8, 4959–5013, 2014

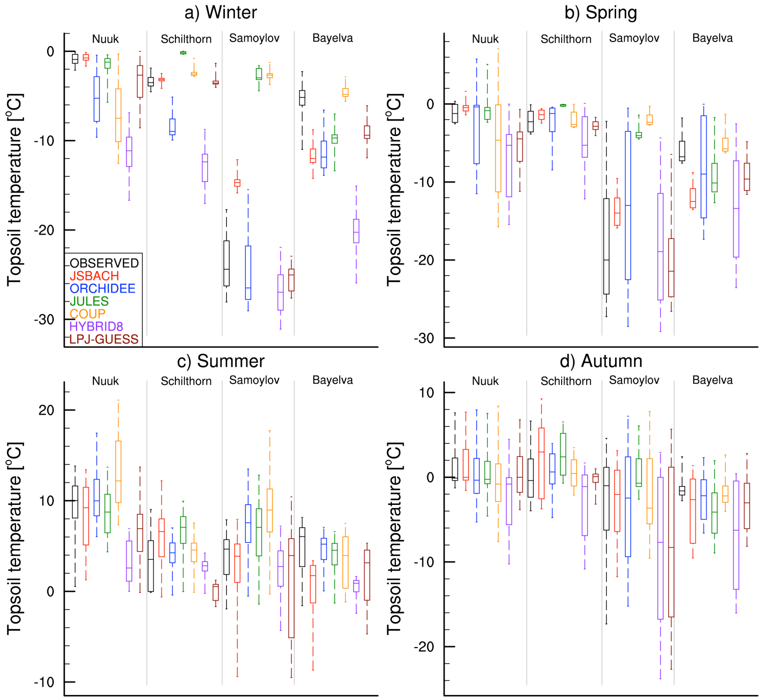

Figure 1. Box plots showing the topsoil temperature for observation and models for different seasons. Boxes are drawn with 25th percentile, mean and 75th percentiles while the whiskers show the min and max values. Seasonal averages of soil temperatures are used for calculating seasonal values. Each plot includes 4 study sites divided by the gray lines. Black boxes show observed values and colored boxes distinguish models. See Table A1 for exact soil depths used in this plot.

TCD
8, 4959–5013, 2014

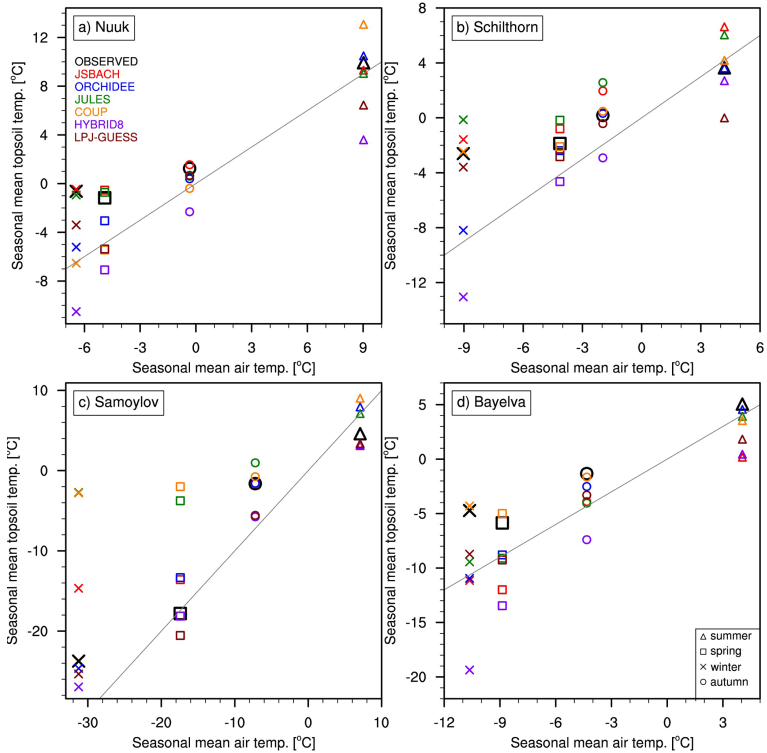

Figure 2. Scatter plots showing air/topsoil temperature relation from observations and models at each site for different seasons. Seasonal mean observed air temperature is plotted against the seasonal mean modeled topsoil temperature separately for each site. Black markers are observed values, colors distinguish models and markers distinguish seasons. Gray lines represent the 1 : 1 line. See Table A1 for exact soil depths used in this plot.

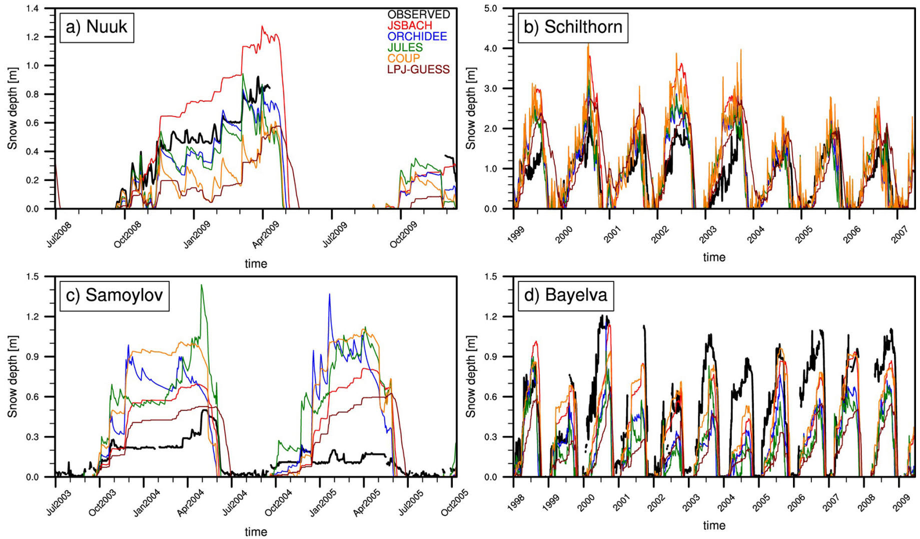

Figure 3. Time series plots of observed and simulated snow depths for each site. Thick black lines are observed values and colored lines distinguish simulated snow depths from models.

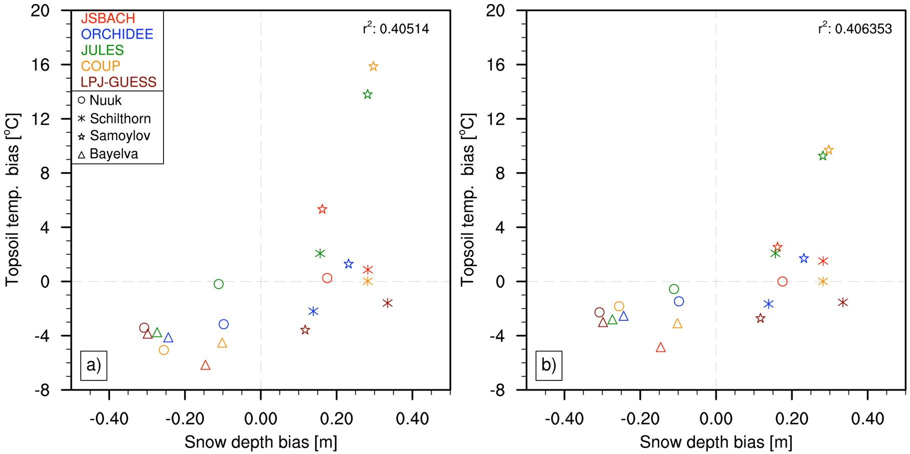

Figure 4. Scatter plots showing the relation between snow depth bias and topsoil temperature bias during snow season **(a)** and the whole year **(b)**. Snow season is defined separately for each model, by taking snow depth values over 5 cm to represent the snow-covered period. The average temperature bias of all snow covered days is used in **(a)**, and the temperature bias in all days (snow covered and snow free seasons) is used in plot **(b)**. Markers distinguish sites and colors distinguish models. See Table A1 for exact soil depths used in this plot.

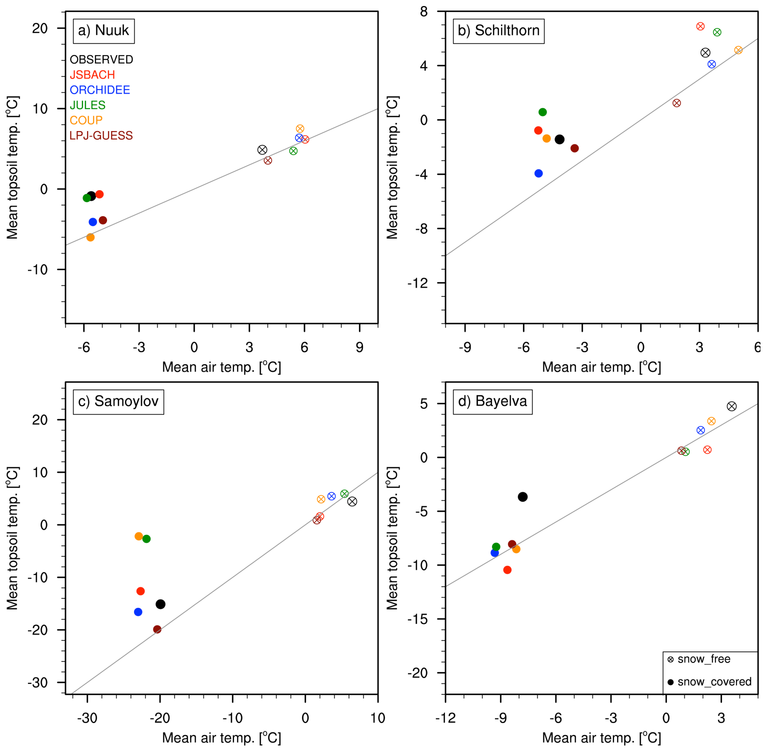

Figure 5. Scatter plots showing air/topsoil temperature relation from observations and models at each site for snow and snow-free seasons. Snow season is defined separately for observations and each model, by taking snow depth values over 5 cm to represent the snow-covered period. The average temperature of all snow covered (or snow free) days of the simulation period is used in the plots. Markers distinguish snow and snow free seasons and colors distinguish models. Gray lines represent the 1 : 1 line. See Table A1 for exact soil depths used in this plot.

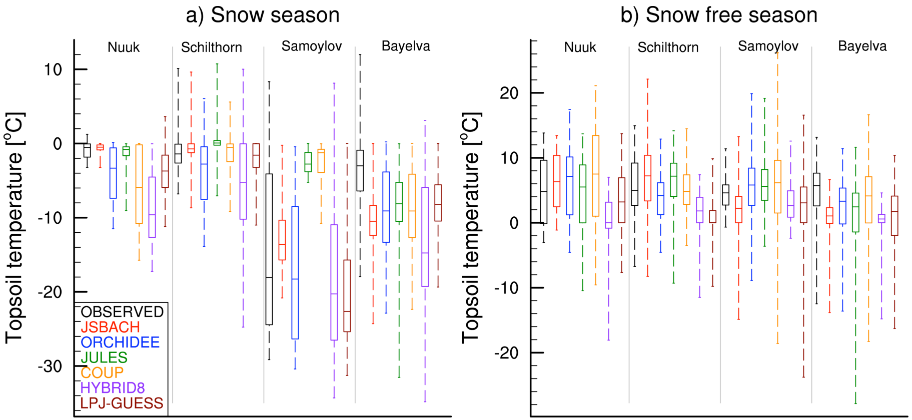

Figure 6. Box plots showing the topsoil temperature for observation and models for snow and snow free seasons. Snow season is defined separately for observations and each model, by taking snow depth values over 5 cm to represent the snow-covered period (observed snow season is used for HYBRID8). Boxes are drawn with 25th percentile, mean and 75th percentiles while the whiskers show the min and max values. Each plot includes 4 study sites divided by the gray lines. Black boxes are observed values and colored boxes distinguish models. See Table A1 for exact soil depths used in this plot.

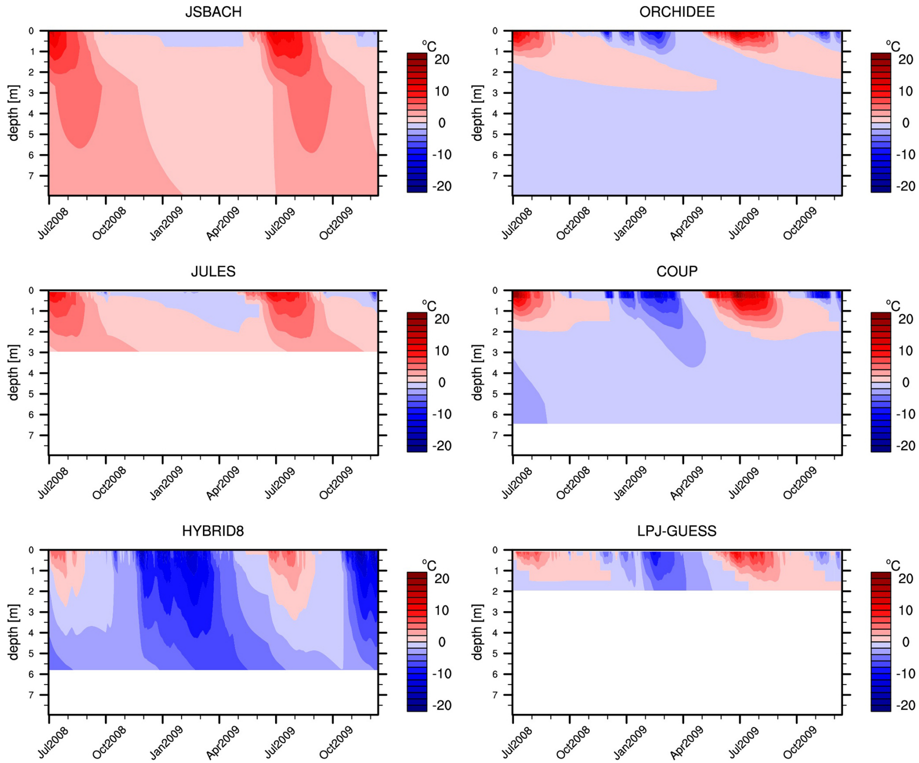

Figure 7. Time-depth plot of soil temperature evolution at the Nuuk site for each model. Simulated soil temperatures are interpolated into 200 evenly spaced nodes to represent a continuous vertical temperature profile. The deepest soil temperature calculation is taken as the bottom limit for each model (no extrapolation applied).

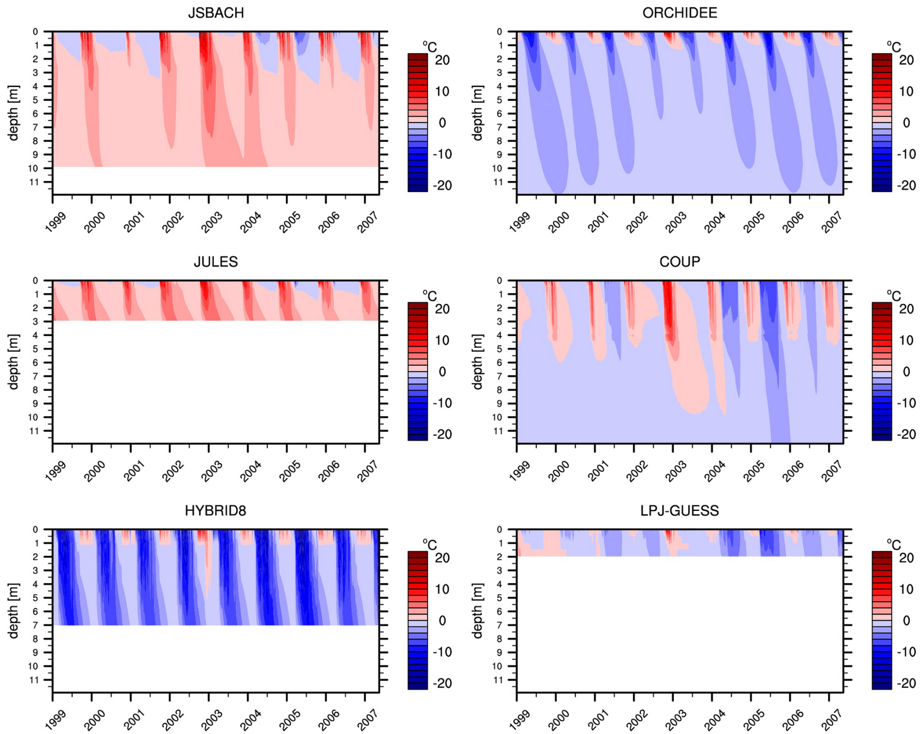

Figure 8. Time-depth plot of soil temperature evolution at Schilthorn site for each model. Simulated soil temperatures are interpolated into 200 evenly spaced nodes to represent a continuous vertical temperature profile. The deepest soil temperature calculation is taken as the bottom limit for each model (no extrapolation applied).

TCD
8, 4959–5013, 2014

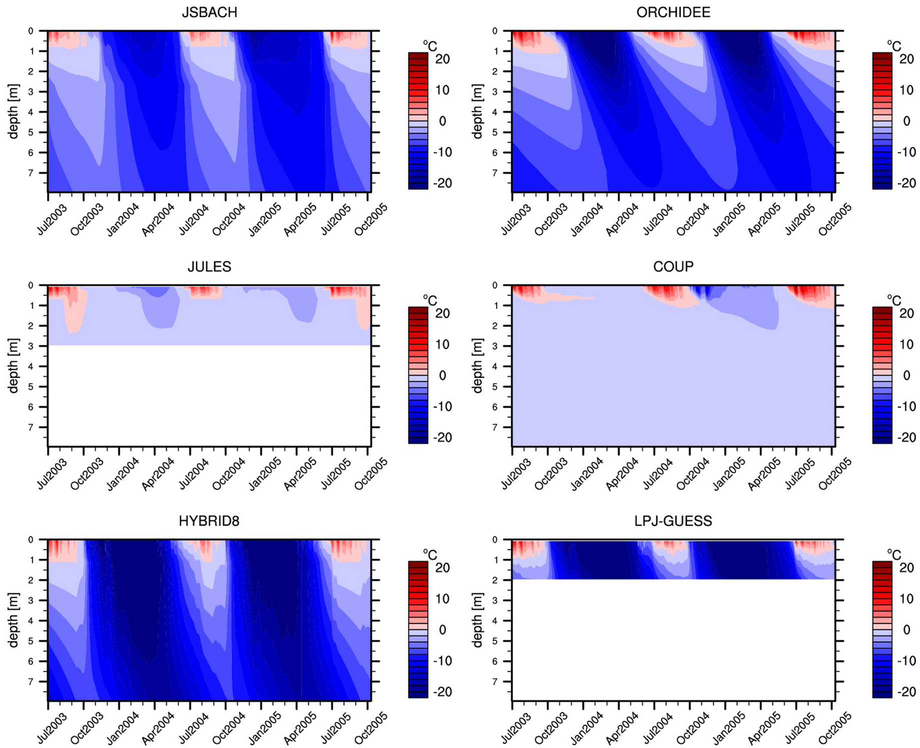

Figure 9. Time-depth plot of soil temperature evolution at Samoylov site for each model. Simulated soil temperatures are interpolated into 200 evenly spaced nodes to represent a continuous vertical temperature profile. The deepest soil temperature calculation is taken as the bottom limit for each model (no extrapolation applied).

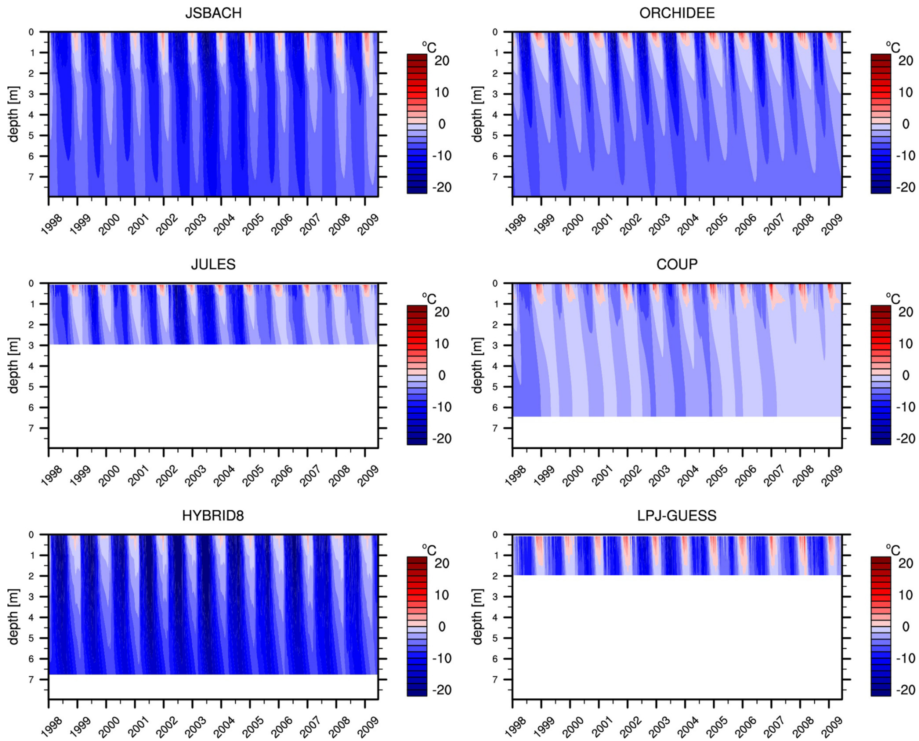

Figure 10. Time-depth plot of soil temperature evolution at Bayelva site for each model. Simulated soil temperatures are interpolated into 200 evenly spaced nodes to represent a continuous vertical temperature profile. The deepest soil temperature calculation is taken as the bottom limit for each model (no extrapolation applied).

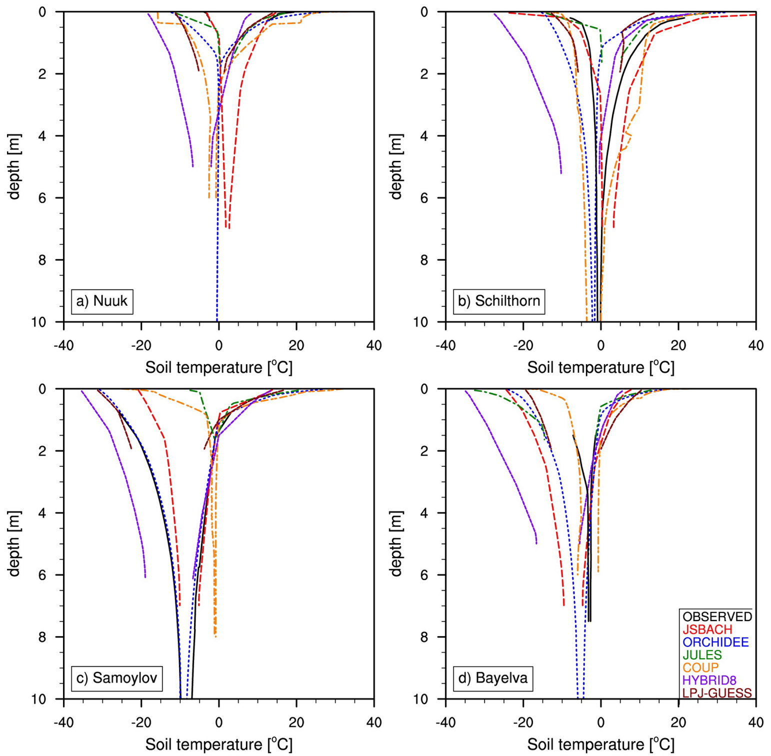

Figure 11. Soil temperature envelopes showing the vertical profiles of soil temperature amplitudes of each model at each site. Soil temperature values of observations (except Nuuk) and each model are interpolated to finer vertical resolution and max and min values are calculated for each depth to construct max and min curves. For each color, the right line is the maximum and the left line is the minimum temperature curve. Black thick lines are the observed values and colored dashed lines distinguish models.

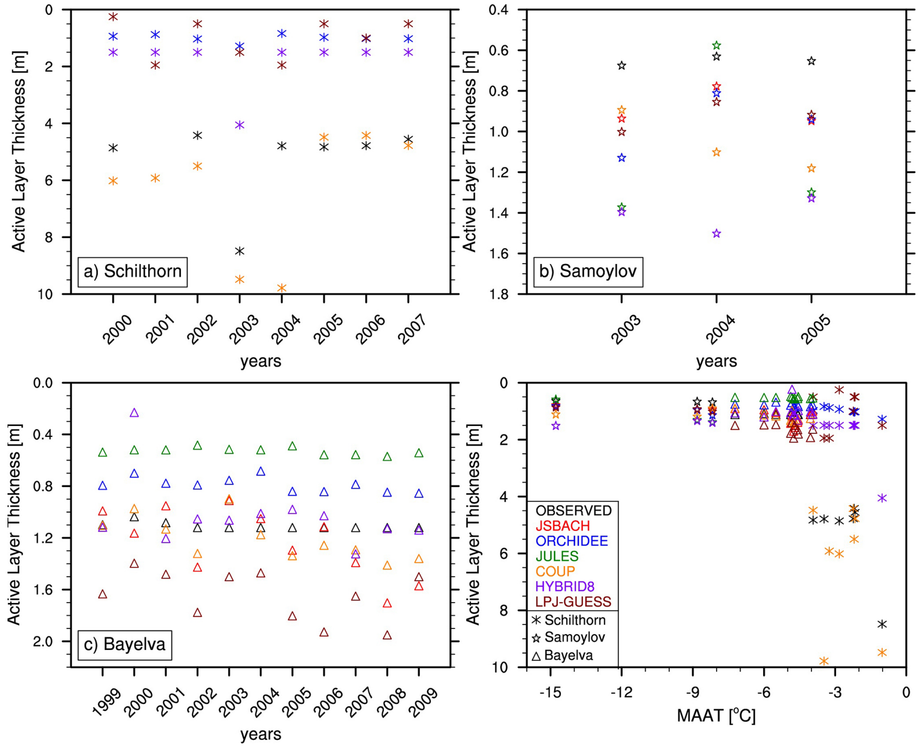

Figure 12. Active layer thickness (ALT) values for each model and observation at the three permafrost sites. ALT calculation is performed separately for models and observations by interpolating the soil temperature profile into finer resolution and estimating the maximum depth of 0 °C for each year. **(a–c)** show the temporal change of ALT at Schilthorn (2001 is omitted because observations have major gaps, also JSBACH and JULES are excluded as they simulate no permafrost at this site), Samoylov and Bayelva respectively, while the lower-right plot shows their relation to mean annual air temperature (MAAT). Colors distinguish models/observations and markers distinguish sites.

TCD
8, 4959–5013, 2014

Site-level model intercomparison of high latitude and high altitude soil thermal dynamics

A. Ekici et al.

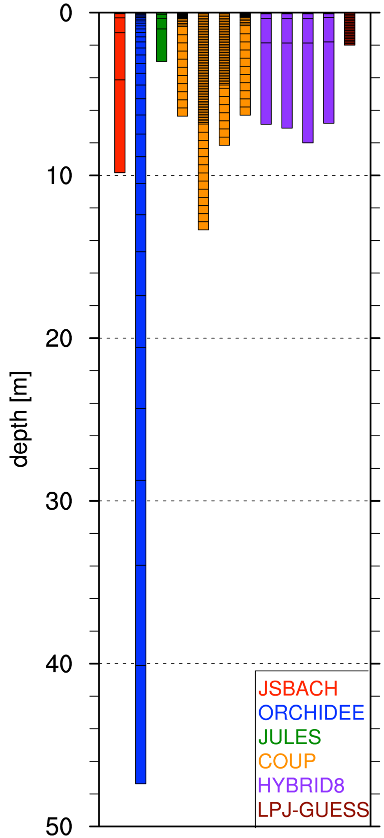

Figure A1. Soil layering schemes of each model. COUP and HYBRID8 models use different layering schemes for each study site, which are represented with different bars (from left to right: Nuuk, Schilthorn, Samoylov and Bayelva).

TCD
8, 4959–5013, 2014